Review article

# *Nanoscale zerovalent* copper (nZVC) catalyzed environmental remediation of organic and inorganic contaminants: A review

Sandeep Kumar [a,*], Parminder Kaur [a], Ravinderdeep Singh Brar [a], J Nagendra Babu [b]

[a] Department of Chemistry, Akal University, Talwandi Sabo, Bathinda, 151302, Punjab, India
[b] Department of Chemistry, School of Basic and Applied Science, Central University of Punjab, Bathinda, 151001, Punjab, India

ABSTRACT

Over the past decade, the nano zerovalent copper has emerged as an effective nano-catalyst for the environment remediation processes due to its ease of synthesis, low cost, controllable particle size and high reactivity despite its release during the remediation process and related concentration dependent toxicities. However, the improvised techniques involving the use of supports or immobilizer for the synthesis of $Cu^0$ has significantly increased its stability and motivated the researchers to explore the applicability of $Cu^0$ for the environment remediation processes, which is evident from access to numerous reports on nano zerovalent copper mediated remediation of contaminants. Initially, this review allows the understanding of the various resources used to synthesize zerovalent copper nanomaterial and the structure of $Cu^0$ nanoparticles, followed by focus on the reaction mechanism and the species involved in the contaminant remediation process. The studies comprehensively presented the application of nano zerovalent copper for remediation of organic/inorganic contaminants in combination with various oxidizing and reducing agents under oxic and anoxic conditions. Further, it was evaluated that the immobilizers or support combined with various irradiation sources originates a synergistic effect and have a significant effect on the stability and the redox properties of nZVC in the remediation process. Therefore, the review proposed that the future scope of research should include rigorous focus on deriving an exact mechanism for synergistic effect for the removal of contaminants by supported nZVC.

## 1. Introduction

Growing demands of industrial goods with the population boom has resulted in an increased discharge of industrial effluents into water streams and soil. In addition, many natural and anthropogenic activities also result in contamination of terrestrial and aquatic environments. These activities release effluents of organic/inorganic origin, which pose serious threats to flora and fauna and have adverse physiological effects on humans and ecosystem (Mahmoud and Gan, 2018). So, there is an urgent need to develop sustainable methods and technologies to treat the municipal waste and industrial effluents enormously loaded with organic and inorganic contaminants. In the past few decades, many conventional and economically non-viable approaches including physical, chemical and biological process have been employed for the remediation of the environment, but the real solution to this problem has been provided by nanotechnology in the form of tailored nanoparticles (Akhtar et al., 2020). The nanoscale zerovalent nanoparticles such as iron ($Fe^0$), cobalt ($Co^0$), nickel ($Ni^0$), copper ($Cu^0$) and zinc ($Zn^0$) etc. owing to their distinct physico-chemical properties and the significant role they played in the removal of various contaminants, have attracted the attention of a large scientific community (Li et al., 2016). The high contaminant removal efficiencies of these nanoscale materials are associated with their high surface area to weight ratios, which renders them high reactivities towards various contaminants in comparison to their microscale metal counterparts (E Guerra et al., 2018). Among these easily available metallic particles, copper has been significantly evaluated in literature for its environment remediation processes due to high abundance, low cost, controllable particle size, high reactivity and tunable redox properties.

Copper ($^{63}Cu_{29}$) is an element derived from its ores like chalcopyrite ($CuFeS_2$, 34.5% Cu), Cuprite ($Cu_2O$, 88.8%), chalcocite ($Cu_2S$, 79.8%), covellite ($CuS$, 66.5%), malachite ($CuCO_3.Cu(OH)_2$, 57.7%) etc. using various electrolytic refining processes (Daehn and Allanore, 2020; Moskalyk and Alfantazi, 2003). Since its discovery around 3500 BC, it found many application ranging from manufacturing of weapons and coins, as alloys with metals like tin (bronze), zinc (brass), Ag (sterling silver), Ni

---

* Corresponding author.
  *E-mail address:* sandeepchem83@gmail.com (S. Kumar).

(cupronickel, constantan) for the making industrial goods etc (Davis, 2001; Powell and Webster, 2019). Due to its high thermal conductivity (401 W m$^{-1}$ K$^{-1}$ at 0 °C) and electro-conductivity (5.96 × 10$^7$ S m$^{-1}$ at 20 °C), it is also used in the manufacturing of thermocouples and electrical devices (Berman and Macdonald, 1952; Dadras and Morris, 1997; Lu et al., 2004; Maki et al., 2013; Minneci et al., 2021; Pickard et al., 2021). Further, with the emergence of field of nanochemistry, and due to its distinct variable oxidation states (Cu$^0$, Cu$^I$, Cu$^{II}$, Cu$^{III}$), copper based nanomaterial found many application in diverse areas such as catalysis viz. electrocatalysis, photocatalysis and organic transformation (Chen et al., 2021; Dong et al., 2019; Gawande et al., 2016; Ojha et al., 2017; Sambiagio et al., 2014; Shi and Buchwald, 2015), plant biology (Lamichhane et al., 2018; Liu et al., 2018; Panagos et al., 2018), medicine (Ahmedova et al., 2018; Mallick and Sabui, 2021) and environment remediation (de Sousa et al., 2019a; Fang and Guo, 2018). However, the pyrophoric nature of Cu$^0$ nanomaterial due to its high sensitivity towards O$_2$ and H$_2$O restrict their application in various fields like optics and electronics etc (Gawande et al., 2016).

Recent studies have confirmed that the advanced techniques and improved methodologies comprising the involvement of immobilizers/ stabilizers have enhanced the stability of Cu$^0$ nanoparticles having core-shell structure (Ali et al., 2018; Huang et al., 2017; Issaabadi et al., 2017; Wang et al., 2017). The redox behavior of Cu$^0$ is very useful in determining the stability and its surface passivation. The Cu$^0$ has inherent stability at negative potential. Further, the oxidation of Cu$^0$ is observed over a wide range of pH; with formation of Cu$^+$ in acidic and neutral solutions and Cu$^{2+}$ at higher pH values. The acidic pH favors the dissolution of Cu$^0$ and formation of thermodynamically favorable species as a product; while the alkaline medium produces a layer of oxide over metal, thus preventing its further corrosion (Beverskog et al., 1997). Thus, the catalytic ability of Cu$^0$ is related to generation of electron and ionic species (Cu$^+$ and Cu$^{2+}$), along with oxides and hydroxides over metal surface while performing the reductive degradation of environment contaminants (Yamaguchi et al., 2018). When present in its lowest oxidation state (Cu$^0$) in the system, it has a strong tendency to involve in redox processes through one-electron transfer (Cu$^+$ + e$^-$ → Cu$^0$, E$^o$ = +0.521 V) or two-electron transfer (Cu$^{2+}$ + 2e$^-$ → Cu$^0$, E$^o$ = +0.342 V) (Oliveira et al., 2018) and thus catalyze a number of homogeneous oxidative coupling reactions (Ojha et al., 2017; Saha and Das, 2018; Sambiagio et al., 2014) or heterogeneous Fenton-like degradation processes (Lu et al., 2004). However, the homogeneous reaction has an associated disadvantage of catalyst consumption and sludge formation (Matavos-Aramyan et al., 2017).

Over the period the researchers have developed heterogeneous Fenton-like reaction systems involving the use of nano zerovalent copper as Fenton catalyst with oxidizing agents like H$_2$O$_2$ (Ma et al., 2018). The catalytic efficiency of nano zerovalent copper was significantly enhanced by the use of porous materials such as zeolite (Danish et al., 2017), green rust (Fang et al., 2019), iron oxide (Kim and Ko, 2018), carbon nanotubes (Zheng et al., 2021), cellulose (Kamal et al., 2019), chitosan Alani et al. (2021) etc. as an immobilizer or support. The catalytic performance of Cu$^0$ is enhanced by catalyst's support via adsorption of contaminants near the active sites and further assistance in generation of radical species and initiation of other pollutant decomposition pathways. In Fenton-like reactions, the rate of generation of free radical species is accelerated by the use of combination of Cu$^0$ catalyst with ultrasound energy (Wang et al., 2019b), microwave radiations (Lee et al., 2010), ultraviolet radiation (Dinesh et al., 2020) along with oxidizing agents such as H$_2$O$_2$ (Liu et al., 2021b) and persulfate (Zhang et al., 2020b), or a combination of these.

Although there are several reports on the preparation of nano zerovalent copper and its application for the environment remediation process, however, no review paper has summarizes the effect of various dependent parameters like concentration of contaminant, dose of nZVC catalyst, pH, and reaction time on the contaminant removal efficiencies

of nZVC. This review comprehensively discuss the effect of various oxidizing/reducing agents, pH of solution, synergistic effect from immobilizers/supports and various energy sources in the activation of nano zerovalent copper to produce the reactive species involved in the catalytic degradation of various organic contaminants or reductive removal of heavy metals. In the first section, the detailed discussion has been carried out on the various strategies involved in the preparation of stable nano zerovalent copper materials. A comprehensive discussion on the structure and mechanism of contaminant removal by nano zerovalent copper has been provided in the second and third section. The fourth section involved the application of nano zerovalent copper for the various organic and inorganic pollutants. The organic pollutants are further categorized into organic compounds, dye and drug molecules, and the various affecting parameters like contaminant concentration, nZVC dose, pH, time and percentage removal efficiencies are summarized in tabular form. The conclusion is mentioned at the end, with the suggestion to understand the underlying mechanism of synergistic effect for the removal of contaminants that may originate between the nano zerovalent copper and the immobilizer/support, as the future perspectives of this review article.

## 2. Synthesis of nZVC

The catalytic efficiencies of nanoparticles as an environment remediating agent are controlled by the size of synthesized nanoparticles, material used as a support, capping material and thickness of surface oxide layer etc (Pasinszki and Krebsz, 2020). Therefore, the synthetic approach used for the manufacturing of nanoparticles plays a very significant role in deciding the properties and application of nano-catalyst obtained (Khodashenas and Ghorbani, 2014). There are generally three major categories of approaches used for the synthesis of nanoparticles namely *chemical, physical, and biological process* (Figure 1). Otherwise the different methods used for the synthesis of metallic nanoparticles includes chemical reduction (Chang et al., 2019), cathodic corrosion (Feng et al., 2018; Yanson et al., 2011), microwave-assisted (Hashimi et al., 2020), reverse-micelle (Gutierrez et al., 2021), laser-irradiation (Shahzeydi et al., 2019), electrochemical (Serra and Valles, 2018), microemulsion (Mdlovu et al., 2018), ultrasound (Sierra-Ávila et al., 2018), thermal decomposition (Numaga et al., 2020) and biogenic synthesis (El-Saadony et al., 2020) etc. The stability of synthesized copper nanoparticles is always of great concern as these can be easily oxidized on contact with air; therefore, these reactions are always performed under an inert atmosphere by purging the reaction vessel with nitrogen or argon gas. Protecting layers of organic and inorganic materials are usually employed to impart stability to nanoparticles and thus to prevent surface oxidation of copper (Begletsova et al., 2018; Kim et al., 2019; Suárez-Cerda et al., 2017). Protective agents like toluene, dodecanethiol, triethylamine, carbon, silicon, polyethylene glycols, polyacrylic acid, sodium dodecyl benzene sulfonate/sodium dodecyl sulfate, lauric acid etc. has been used in literature to prevent oxidation and thus to prepare stable copper nanoparticles (Khodashenas and Ghorbani, 2014).
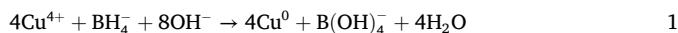
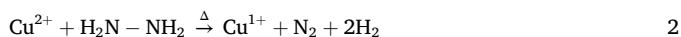### 2.1. Chemical process

#### 2.1.1. Chemical reduction process

Among the various processes used for the synthesis of metallic copper, the chemical reduction of aqueous copper salts using reducing agents such as sodium borohydride (NaBH$_4$), hydrazine (N$_2$H$_4$), sodium hypophosphite (NaPO$_2$H$_2$), and ascorbic acid (vitamin C) etc. has been the most commonly employed method in literature due to its economic viability, repeatability, uniform particle size distribution and easy to perform experimental conditions.

*Reduction using NaBH$_4$*: Theoretically speaking, the stoichiometric ratio required for the reduction reaction of Cu$^{2+}$ using NaBH$_4$ is 4:1 (Eq. 1). When the NaBH$_4$ concentration dependent synthesis of Cu(0)
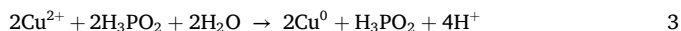
was performed with lower $NaBH_4$ concentrations, $Cu_2O$ and $Cu(OH)_2$ were obtained as intermediates for the reduction process, which were further confirmed by XRD analysis (Liu et al., 2012). With increase in concentration of $NaBH_4$, the peak respective of $Cu(OH)_2$ disappeared, however the $Cu_2O$ contamination was removed only when the concentration of $NaBH_4$ reaches 8 times higher than that of the required stoichiometric dosage. Further, the decrease in size of copper nanoparticles was observed with increase in the dosage of $NaBH_4$ for the reduction process.
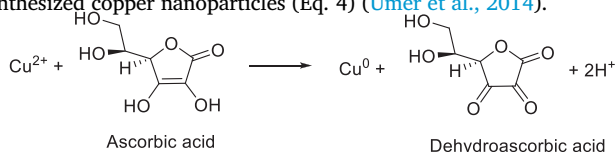
$$4Cu^{4+} + BH_4^- + 8OH^- \rightarrow 4Cu^0 + B(OH)_4^- + 4H_2O \qquad 1$$

*Reduction using hydrazine*: Hydrazine reduces the Cu(II) to Cu(I) at room temperature, however, at elevated temperature it converts Cu(I) to Cu(0). Nitrogen gas released during the process provides an inert atmosphere for the reduction process (Eq. 2) (Andal and Buvaneswari, 2017; Behera and Giri, 2014).

$$Cu^{2+} + H_2N - NH_2 \xrightarrow{\Delta} Cu^{1+} + N_2 + 2H_2 \qquad 2$$

*Reduction using sodium hypophosphite*: Sodium hypophosphite reduces Cu(II) to Cu(0) under acidic conditions in the presence of a number of capping and stabilizing agents (Eq. 3) (Lai et al., 2013; Zhu et al., 2005). Acidic condition favors the activation of sodium hypophosphite and prevents the formation of $Cu(OH)_2$.

$$2Cu^{2+} + 2H_3PO_2 + 2H_2O \rightarrow 2Cu^0 + H_3PO_2 + 4H^+ \qquad 3$$

*Reduction using ascorbic acid*: L-Ascorbic acid not only reduces the Cu(II) to Cu(0), but also act as capping agent and provides stability to the synthesized copper nanoparticles (Eq. 4) (Umer et al., 2014).



### 2.1.2. Thermal decomposition

High temperature and pressure in a closed vessel, usually an autoclave, results in decomposition of aqueous salt of copper to copper nanoparticles. Seku et al. (2018) synthesized copper nanoparticles (average size 14 nm) with *kondagogu* a carboxymethyl gum as a capping agent using hydrothermal synthesis. Zhou et al. (2015) used supercritical hydrothermal synthesis to prepare nZVC with size ranging from 14-50 nm. Solvothermal methods have also been used for the synthesis of supported copper nanoparticles. Xu et al. (2018) used ethanol as solvent for one-pot solvothermal method for the synthesis of metallic copper doped ZnO microrods. In another solvothermal method using ethanol, Li et al. (2014) prepared copper nanoparticles supported on $Li_4Ti_5O_{12}$ composites for use in Li-ion batteries. Chen et al. (2010) used facile hydrothermal method for the synthesis of metallic copper nanoparticles with morphologies like spherical, nanocubes and ribbon-like network using SDBS as stabilizer. Rahmatolahzadeh et al. (2017) used ethylenediamine and hydrazine hydrate for the facile hydrothermal synthesis of *Cu nanoparticles* with average size of 15 nm. Kumar et al. (2022) used one-pot facile hydrothermal synthesis of copper nanowires using oleylamine and oleic acid as stabilizers.

### 2.1.3. Electrochemical synthesis

In electrochemical method of synthesis, the electric current is passed between two electrodes dipped in an aqueous solution of copper salt and sulfuric acid as an electrolyte. The synthesis of nanoparticles is observed at the electrode/electrolyte interface. Balasubramanian et al. (2017) used electrochemical deposition technique to prepare copper nanoparticles supported on reduced graphene oxide.

### 2.1.4. Photochemical reduction

Reduction of aqueous copper ions to copper nanoparticles can be achieved using various forms of electromagnetic radiations. The intensity of light, nature of sensitizer and concentration of stabilizer/support are the determining factors for the size of copper nanoparticles. Kapoor et al. (2003) prepared copper nanoparticles under UV light using
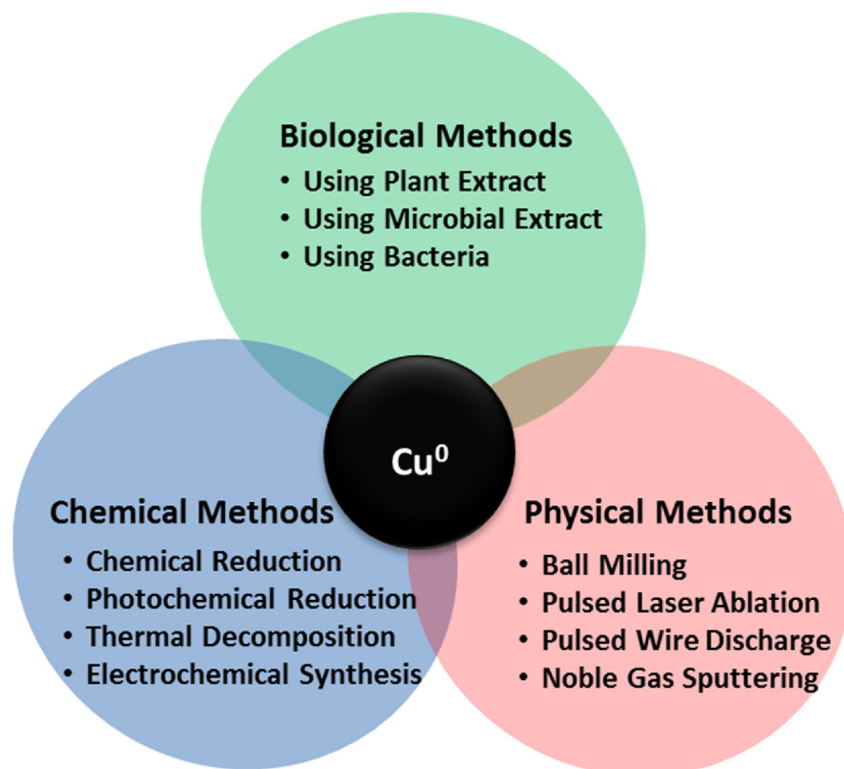


**Figure 1.** Synthetic approaches for the preparation of nZVC nanomaterial.

benzophenone as a photo-sensitizer and poly(N-vinylpyrrolidone) as a stabilizing agent. Wan et al. (2021) prepared ultra-small copper nanoparticles onto the surface of fullerenol using photoreduction method. Microwave is another form of electromagnetic energy with frequency range from 300 MHz to 300 GHz (Zhu et al., 2004). Kamal et al. (2019) performed microwave assisted synthesis of copper nanoparticles stabilized on carboxymethyl cellulose and bacterial cellulose as support.

## 2.2. Physical process

Physical process used for the synthesis of copper nanoparticles involves top-down approach, in which the size of bulk copper is reduced to nanoscale using various mechanical processes such as milling, pulsed laser ablation, etching, and noble gas sputtering etc.

### 2.2.1. Ball milling method

Ball milling is the economical method used for industrial scale production of nanoparticles and is the most commonly employed physical process for conversion of millimeter sized copper fillings to nanosized copper using stirred ball mills. Capping agents are added during the milling process to prevent the oxidation of copper nanoparticles. Further, the milling speed, temperature, time, type of vessel, atmosphere, and stabilizing agent decides the size and properties of the prepared copper nanoparticles.

### 2.2.2. Pulsed laser ablation

Pulsed laser ablation technique involves the degradation of a solid copper in an inert atmosphere in a closed chamber under vacuum upon irradiation with a high energy laser beam to form plasma, which on cooling in the presence of solvent give a colloidal solution (Sadrolhosseini et al., 2019). The quality of the nanoparticles is influenced by the type of solvents used for the ablation, intensity of laser beam and duration of pulsing etc. Tyurnina et al. (2014) used pulsed laser irradiation (wavelength - 1064 nm, duration - 100 ns) for the synthesis of stable colloidal solution of copper nanoparticles. Goncharova et al. (2019) also used pulsed laser radiation for a duration of 7 ns for the synthesis of copper nanoparticles and studied the role of different solvent systems like

ethyl alcohol, NaOH and $H_2O_2$ in deciding the morphology of the prepared nanoparticles.

### 2.2.3. Pulsed wire discharge method

This method is applied to metals with high ductility and electrical conductivity. Due to its high cost and effectiveness for fewer metals, this method has limited industrial applications for the synthesis of nanomaterial. Tokoi et al. (2013) synthesized copper nanoparticles from copper wire in deionized water by applying power ranging from 0.8 to 5.5 kV. Murai et al. (2007) prepared copper nanoparticles (size 10–25 nm) with organic coating via evaporation of copper by wire explosion method in oleic acid mist. In another method *Cu nanoparticles* of size 16–43 nm were synthesized by applying power of 22 kV under a pressure of 0.1 MPa (Dash and Balto, 2011).

### 2.2.4 Noble Gas Sputtering

Inert-gas condensation method has been used to prepare copper nanoparticles based on DC magnetron sputtering using noble gases like Ar or He. Soganci et al. (2018) prepared copper nanoparticle decorated graphene using noble gas sputtering technique with average particle size of 5 nm. Dong et al. (2018) decorated $TiO_2$ nanotube arrays with *Cu nanoparticles* through magnetron sputtering using Ar gas under pressure (10 mTorr).

## 2.3. Biological process

Other than chemical and physical processes, the green method of obtaining metallic copper has also been successfully explored owing to their low cost and eco-friendly nature bearing no adverse impacts on the environment (Suresh et al., 2013) (Figure 2). The green method involves the use of plant extracts or metabolic activities of microorganisms like bacteria and fungi for the reduction of $Cu^{II}$ to $Cu^0$ (Thiruvengadam et al., 2019).

### 2.3.1. Using plant extract

Bio-extracts obtained from various plant parts (leave, stem, bark, root etc.) includes metabolites such as alkaloids, flavonoids, terpenoids,
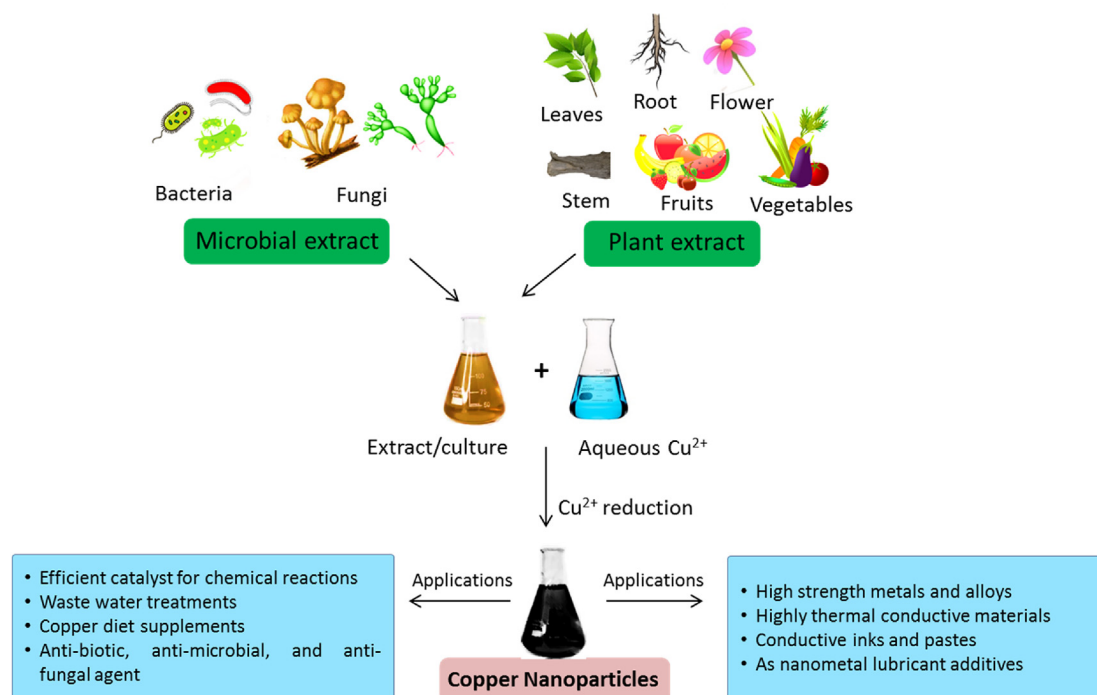


**Figure 2.** Green synthesis of copper nanoparticle.

polyphenols, proteins etc., not only acts as reducing agent, but also stabilizes the produced nanoparticle by providing a protective capping onto it. Different bio-extracts used for the synthesis of copper nanoparticles includes *Eucalyptus camaldulensis* (river red gum) (Asghar and Asghar, 2020)*, Murraya koenigii* (curry tree) (Pantawane et al., 2020; Pragyan and Pragnya, 2019)*, Azadirachta indica* (neem) (Abhiman et al., 2018; Nagar and Devra, 2018)*, Avicennia marina* (grey mangrove) (Essa et al., 2021)*, Datura stramonium* (jimsonweed) (Parikh et al., 2014)*, Rosa rubiginosa* (sweet briar) (Asghar and Asghar, 2020)*, Magnolia kobus* (Lee et al., 2013)*, Cissus arnotiana* (Rajeshkumar et al., 2019)*, Terminalia arjuna* (arjun tree) (Sharma and Gupta, 2021; Yallappa et al., 2013)*, Citrus limon* (lemon) (Amer and Awwad, 2021)*, Syzygium aromaticum* (Clove) (Rajesh et al., 2018)*, Eclipta prostrata* (false daisy) (Chung et al., 2017)*, Ginkgo biloba* (Nasrollahzadeh and Sajadi, 2015)*, Punica granatum* (pomegranate) (Padma et al., 2018) etc.

### 2.3.2. Using microbial extract

Extracts from cultured microorganisms like fungi and bacteria have been used for the synthesis of metallic copper (Varshney et al., 2010).

### 2.3.3. Using bacteria

Prokaryotes such as bacteria owing to their ease of culture, high multiplication rate and optimum culture condition has been used for biogenic synthesis of copper nanoparticles (Shobha et al., 2014). *Morganella psychrotolerans* and *Morganella morganii* RP42 were used for the synthesis of nZVC with particle size in the range of 15–20 nm (Ramanathan et al., 2011, 2013). Varshney et al. (2010) employed a rapid biological process to synthesize copper nanoparticles (size 8–15 nm) using *Pseudomonas stutzeri*, a non-pathogenic bacterium. In another study, Varshney et al. (2011) also utilized *Pseudomonas stutzeri* to synthesize cubic shaped copper nanoparticles (size 50–150 nm) using wastewater from electroplating process.

### 2.3.4. Using algae and fungi

Fungi secrete a large number of enzymes such as NADH and NADPH during their metabolic processes, and thus play a significant role in the biosynthesis of copper nanoparticles (Noor et al., 2020). The different algal and fungal species used for the synthesis of *Cu nanoparticles* includes *Penicillium aurantiogriseum*, *Penicillium waksmanii* and *Penicillium citrinum* (Honary et al., 2012), *Fusarium oxysporum* (Majumder, 2012), *Hypocrea lixii* (Salvadori et al., 2013), *Bifurcaria Bifurcata* (Abboud et al., 2014), *Trichoderma koningiopsis* (Salvadori et al., 2014), *Chlamydomonas reinhardtii* (Žvab et al., 2021), *Botryococcus braunii* (Arya et al., 2018) etc.

## 3. Structure of nZVC

The typical structure of nZVC prepared using a bottom-up approach consists of a core-shell structure having zerovalent metallic copper as the core and an oxide shell consisting of $Cu_2O$ and CuO (Kim et al., 2013; Liu et al., 2019). The surface oxidation is inevitable due to the pyrophoric nature of copper nanoparticles, until they are synthesized and stored in an inert atmosphere (Alymov et al., 2018). The nZVC core acts as the powerhouse of electrons. The transfer of charge from core through intermediate semiconducting copper oxide layer causes reductive degradation of contaminants on the surface of core-shell nanoparticles (Fathima et al., 2018; Shikha et al., 2015). Stabilizers and capping agents prevent the surface oxidation and thus render extra stability to the nano zerovalent copper (Din and Rehan, 2017). Protective agents like toluene, dodecanethiol, triethylamine, carbon, silicon, polyethylene glycols, polyacrylic acid, sodium dodecyl benzene sulfonate/sodium dodecyl sulfate, lauric acid etc. has been used in literature to prevent oxidation and thus to prepare stable copper nanoparticles (Khodashenas and Ghorbani, 2014). Kim et al. (2013) prevents the surface oxidation of nZVC through the formation of copper–copper formate core–shell nanoparticles. Organic/inorganic support employed for the immobilization provides extra stability to the synthesized nZVC via minimization of aggregation

and leaching of Cu(I/II) under unfavorable conditions. The various organic/inorganic materials used as support for the synthesis of nZVC includes zeolite (Danish et al., 2017), $Fe_2O_3$ (Kim and Ko, 2018), green rust (Fang et al., 2019), $ZrSiO_4$ (Mahmoud et al., 2021), microscale zinc (Li et al., 2020), chitosan (Wu et al., 2009), $TiO_2$ (Alani et al., 2021), cellulose filter paper (Kamal et al., 2016), carboxymethyl cellulose (Kamal et al., 2019), carbon nanotubes (Zheng et al., 2021), biochar (Din et al., 2021), graphene (Chi et al., 2019; Xu et al., 2019), montmorillonite (Hong et al., 2017), pistachio shell powder (Kumar et al., 2021) etc. The experimental conditions and the amount of the supporting materials decide the size and surface area of the synthesized zerovalent copper nanoparticles.

## 4. Mechanism of contaminant removal

Depending on the studies performed to identify the species of copper involved in the removal of various organic/inorganic contaminants, it has been observed that there are mainly three removal processes whereby the copper nanoparticles has been involved in environment remediation phenomenon namely reductive degradation, oxidative removal, and surface adsorption (de Sousa et al., 2019a). In the absence of dissolved oxygen (anoxic), the removal process primarily involves the transfer of electrons from $Cu^0$, resulting in reductive degradation/removal of organic/inorganic contaminants. Further, the stability of $Cu^0$ remains intact in the absence of oxygen owing to suppression of hydroxyl radical formation. Conversely, the presence of oxygen (oxic) generates various reactive oxygen species (ROS) like $H_2O_2$, $^1O_2$, $O_2^{\cdot-}$, $\cdot OH$ etc. via transfer of electrons from $Cu^0$, which further causes oxidative degradation of organic contaminants (Wen et al., 2014) (Figure 3). Different radical scavengers have been studied to find the key radical species involved in the degradation mechanisms. In studies, tert-butyl alcohol (TBA) inhibits hydroxyl radicals ($\cdot OH$) (Qi et al., 2016; Wang et al., 2019), superoxide dismutase (SOD) inhibits superoxide anions ($O_2^{\cdot-}$) (Dror et al., 2020), sodium azide ($NaN_3$) inhibits singlet oxygen ($^1O_2$) (Gao et al., 2021), catalase (CAT) was used to identify hydrogen peroxide $H_2O_2$ (Shen et al., 2017), combination of isopropanol with TBA was used to ascertain the type of hydroxyl radical in degradation process (Ma et al., 2018) etc.

The pH of the reaction mixture contributes significantly in deciding the mechanism of the contaminant removal process. At lower pH (less than 7), the $Cu^+$ species predominates in the solution, which promotes *in-situ* generation of $H_2O_2$ from dissolved $O_2$ and $H_2O$ in a Fenton-like process, and later on also participate in the decomposition of $H_2O_2$ to $\cdot OH$ radicals, thus controlling the overall degradation process (Xu et al., 2019). At higher pH (more than 7), the removal of contaminants via surface adsorption prevails due to the formation of copper oxides (CuO) and copper hydroxides ($Cu(OH_2)$) on the surface of copper nanoparticles (Ourique et al., 2018). External oxidizing agents like hydrogen peroxide (Ma et al., 2018), peroxymonosulfate (Zhou et al., 2016) etc. and reducing agents like sodium borohydride (Raut et al., 2016) etc. have also been studied with zerovalent copper for the various degradation processes.

## 5. Applications of nZVC for environment remediation

### 5.1. Removal of organic contaminants

Organic contaminants or waste are the compounds comprising carbon, hydrogen along with other heteroatoms. These contaminants depending on their physical nature may exist in the environment as gas or liquid phase (volatile organic compounds, VOCs) or in solid phase (chemicals, waxes, plastics, resins etc.). Because of their unwanted toxicity associated with their complex structure, they always pose a great threat to flora and fauna. Researchers across the world are working restlessly to develop new methods and state of art techniques to find a solution to this problem. Tailored nanoparticle mediated
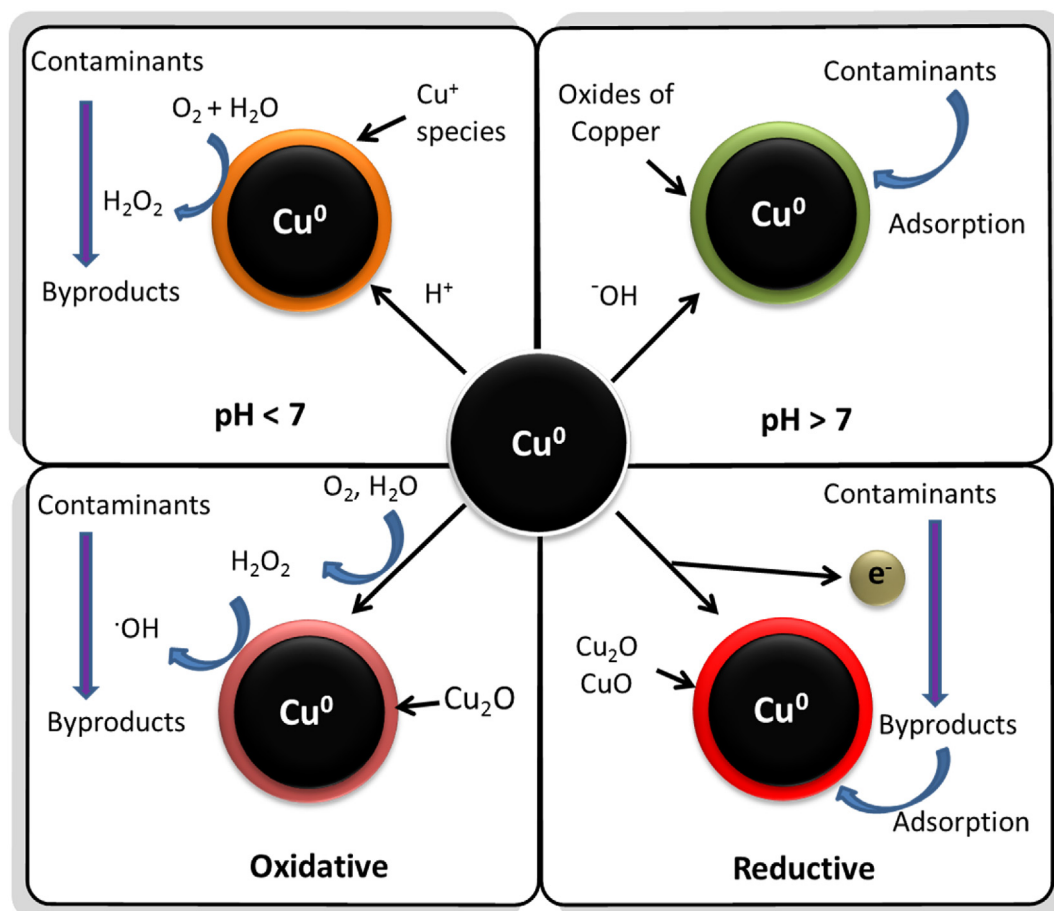
**Figure 3.** Schematic of various mechanisms involved in nZVC mediated contaminant removal processes.

degradation of organic contaminants provide a sustainable and long term solution. Zerovalent copper is one such promising material used in literature for the remediation of organic and inorganic contaminants. So this part of the review will focus on the reports discussing the application of zerovalent copper for the removal of organic contaminants (Table 1).

### 5.1.1. Chlorinated organic compounds (COCs) as pollutants

Chlorinated organic compounds (COCs) are the most common terrestrial contaminants having anthropogenic origin and used for different applications, such as degreasing, dry cleaning, and pesticides. Due to their toxic and persistent nature, these cause a major threat to the environment.

**Table 1.** nZVC mediated removal of organic contaminants.

| nZVC (bare or supported) | Pollutant | Oxidizing /Reducing agent (Conc.) | Optimum experimental conditions | | | | Removal (%) | Ref. |
|---|---|---|---|---|---|---|---|---|
| | | | nZVC dose | Pollutant conc. | pH | Time | | |
| Bare | Dichloromethane | $NaBH_4$ (1 $g \cdot L^{-1}$) | $2.5 g \cdot L^{-1}$ | 26.4 $mg \cdot L^{-1}$ | - | 1h | 90% | (Huang et al., 2012) |
| Reduced $B_{12}$ | Dichloromethane | - | 0.1 $g \cdot L^{-1}$ | 26 $mg \cdot L^{-1}$ | - | 2h | 99% | (Huang et al., 2013) |
| Bare | 2,4-Dichlorophenol | - | 2 $g \cdot L^{-1}$ | 7.5 $mg \cdot L^{-1}$ | 6.2 | 5 days | 67.1% | (Chang et al., 2019) |
| Bare | Monochloro-aromatics | $NaBH_4$ (1.0 $g \cdot L^{-1}$) | 2.5 $g \cdot L^{-1}$ | 34 $mg.L^{-1}$ | 9.5 | 12h | 100 % | (Raut et al., 2016) |
| Bare | 1,2-Dichloroethane | $NaBH_4$ (0.95 $g \cdot L^{-1}$) | 2.5 $g \cdot L^{-1}$ | 30 $mg \cdot L^{-1}$ | - | 2h | 80% | (Huang et al., 2011) |
| Green rust | Tetrabromo-bisphenol A | - | 0.5 $g \cdot L^{-1}$ | 15 $mg \cdot L^{-1}$ | 8 | 5h | 92.11% | (Fang et al., 2019) |
| Zeolitic imidazolate framework | p-Nitrophenol | $NaBH_4$ (6.6 $g.L^{-1}$) | 1.5 $g \cdot L^{-1}$ | 25 $mg \cdot L^{-1}$ | - | 2 min. | 100 % | (Yang et al., 2019) |
| Bare | Benzoic acid | PMS (1 mM) | 40 $mg \cdot L^{-1}$ | 4.9 $mg.L^{-1}$ | 3 | 10 min. | 100 % | (Zhou et al., 2016) |
| Zeolite | Trichloroethylene | SPC (47.1 $g \cdot L^{-1}$) | 0.2 $g \cdot L^{-1}$ | 19.7 $mg \cdot L^{-1}$ | - | 2h | >95% | (Danish et al., 2017) |
| Bare | Diethyl phthalate | - | 0.5 $g \cdot L^{-1}$ | 10 μM | 2.5 | 2h | 100% | (Wen et al., 2014) |
| Bare | 4-Chlorophenol | - | 100 $g \cdot L^{-1}$ | 40 $mg \cdot L^{-1}$ | 3 | 4h | 65% | (Duan et al., 2016) |
| Bare | aniline | $O_3$ (10 $mg \cdot L^{-1}$) | 2 $g \cdot L^{-1}$ | 10 $mg.L^{-1}$ | 6 | 24 min. | 98% | (Zhang et al., 2017a) |
| Bare | Bisphenol AF | PS (0.27 $g \cdot L^{-1}$) | 0.5 $g \cdot L^{-1}$ | 6.7 $mg \cdot L^{-1}$ | 4.0 | 20 min. | 97.0% | (Wang et al., 2019) |
| Bare | Ether amine surfactant | Ascorbic acid (88.1 $g \cdot L^{-1}$) | 60 $mg \cdot L^{-1}$ | 180 $mg \cdot L^{-1}$ | 6 | 4 h | 57% | (Martins et al., 2021) |
| ZrSiO$_4$@NPANI | Nitroanilines | $NaBH_4$ (1 $g \cdot L^{-1}$) | 300 μL | 27.6–69 $mg \cdot L^{-1}$ | 7 | 6–9 min. | 98.4% | (Mahmoud et al., 2021) |
| Microscale zinc | 4-Nitrophenol | - | 2.34 $g \cdot L^{-1}$ | 6.6 $mg \cdot L^{-1}$ | 2.5 | 60 min. | 77% | (Li et al., 2020) |

Dichloromethane (DCM) **1** is an industrial origin organic contaminant known for its high carcinogenicity and hepatotoxic effects. Zerovalent metallic nanoparticles are known for the treatment of chlorinated organic contaminants (COCs) such as tri- and tetrachloromethane, but are found less effective for dichloromethane and dichloroethane probably due to their relatively stronger carbon-chlorine bonds compared to higher-chlorinated organic compounds (Doong et al., 2003; Feng et al., 2005; Wang et al., 2009). However, zerovalent copper (ZVC) was observed as an effective catalyst for dechlorination reactions of dichloromethane under $NaBH_4$ reduction conditions owing to its small size (50 nm) and high surface area (19 $m^2$ $g^{-1}$) (Huang et al., 2012). Under optimized conditions with 2.5 $g \cdot L^{-1}$ of ZVC and 1 $g \cdot L^{-1}$ of $NaBH_4$, nearly 90% of DCM (26.4 $mg \cdot L^{-1}$) was degraded within 1 h of reaction time. Chloride ions were the immediate product of the degradation reaction as indicated by IC analysis of the reaction mixture. The pseudo-first-order rate constant value (2.19 h) was found to be 2–3 times higher for the ZVC mediated dechlorination of DCM as compared to the other zerovalent metals. Further, the concentration of the leached copper ions in solution was within the permissible limit (2 $mg \cdot L^{-1}$) for drinking water as per WHO standard. Lin et al. (2005) used cation resin supported zerovalent copper nanocomposite for the effective removal of carbon tetrachloride ($CCl_4$) from wastewater. Cation resin not only prevents the agglomeration of ZVC particles, but also adsorbs the $CCl_4$ on its surface to facilitate the removal process. Further, the exchange between $Cu^{2+}$ and $H^+/Na^+$ on the resin, keeps the solution pH between 3 and 4, favorable for the $CCl_4$ dechlorination and $Cu^{2+}$ concentrations less than 0.1 $mg \cdot L^{-1}$.

Vinyl chloride monomer (VMC) is used for the synthesis of polyvinyl chlorides (PVC), a versatile material with several industrial applications (Endo, 2002). 1,2-Dichloroethane (1,2-DCA) **2** is used for the synthesis of vinyl chloride (Liang et al., 2019) and usually the groundwater nearby the VCM industrial plants has been found contaminated with 1,2-DCA (Wang et al., 2015). Huang et al. (2011) used zerovalent copper nanoparticles for the effective remediation of 1,2-DCA using $NaBH_4$ as electron donor. The 1,2-DCA (30 $mg \cdot L^{-1}$) degradation efficiency of more than 80% was observed within 2 h using optimum ZVC dose of 2.5 $g \cdot L^{-1}$ and borohydride concentration of 25 mM. Measured oxidation-reduction potential revealed higher negative values (−1100 eV) with increasing $NaBH_4$ concentrations indicating strong reducing conditions prevailed during reaction. When used individually, neither ZVC nor $NaBH_4$ could degrade/reduce 1,2-DCA. Formation of ethane as the major product (79%) of the 1,2-DCA degradation suggests ZVC mediated two successive hydrogenolysis reactions as a major reaction pathway. The formation of ethylene as the minor product (1%) indicates the presence of dihaloelimination also as the part of degradation reaction.

Huang et al. (2013) evaluated the Cu–$B_{12}$ system for its synergistic effect for the degradation of DCM using Tri-citrate as a reducing agent. The ZVC acts as electron donor and vitamin $B_{12}$ performs the role of electron mediator in the overall reductive degradation process of DCM. Batch experiments performed to study the degradation process showed that nearly 99% of the DCM (26 $mg \cdot L^{-1}$) was degraded reductively to give methane and methyl chloride as products within 2 h of reaction time by Cu –$B_{12}$ system, which was significantly higher than that of using $B_{12}$ alone. The rate of DCM degradation was observed to be a function of ZVC dose and increases rapidly with increase in ZVC concentration (<0.1 $g \cdot L^{-1}$). Tri-citrate mediated reduced form of $B_{12}$ was responsible for the DCM degradation on the surface of ZVC. The pseudo first order rate of reaction was observed with a rate constant of 1.35 $h^{-1}$, which was higher (5 times) than that of vitamin $B_{12}$ when used alone.

Chang et al. (2019) investigated the degradation efficiencies of zerovalent copper nanoparticles (Cu-GT NPs) synthesized via green approach using green tea extract towards the organic contaminant 2,4-dichlorophenol (2,4-DCP) **3** and a comparison was performed with the chemically synthesized zerovalent copper (Cu-SB) nanoparticles for their physico-chemical properties. The particle sizes of 5 nm and 200 nm were determined using dynamic light scattering (DLS) technique for Cu-GT NPs and Cu-SB, respectively. The Cu-SB nanoparticles were observed to possess higher reducibility and reactivity than Cu-GT NPs. Higher reductive degradation efficiencies (67.1%) of 2,4-DCP (7.5 ppm) observed with Cu-SB (2 $g \cdot L^{-1}$) at near neutral pH (6.2) with incubation period of 5 days instead of its lower dispersion and stability compared to Cu-GT NPs was ascribed to the higher activation energy of Cu-SB particles (29.65 kJ $mol^{-1}$) for 2,4-DCP degradation. Further, the lower reactivity of Cu-GT NPs was associated with formation of a high percentage of monovalent copper. Lee et al. (2010) compared the nZVC mediated degradation of chlorobenzene (Cl–B) **4** in the presence and absence of microwave (MW) energy. The MW energy directly generates the heat inside the nZVCs that causes an increase in CB degradation efficiency (1.8 times) from 19.5% to 41.3% by decreasing the activation energy from 21.4 kJ $mol^{-1}$ to 15.8 kJ $mol^{-1}$.

Raut et al. (2016) evaluated the degradation efficiencies of zerovalent copper nanoparticles synthesized via chemical reduction using sodium borohydride for the monochloro-aromatic compounds such as chlorobenzene (Cl–B) **4**, chloropyridine (Cl-Py) **5**, chlorotoluene (Cl-T) **6** and chlorobiphenyl (Cl-BPh) **7**. Under the optimized conditions using ZVC nanoparticles (2.5 $g \cdot L^{-1}$) and $NaBH_4$ (1.0 $g \cdot L^{-1}$) as reducing agents, nearly 100% dechlorination was observed for all chloro-aromatics within 12 h. GCMS and NMR techniques were used to analyze the reaction intermediate and dechlorinated products to determine the reaction pathway. Acidified isopropyl alcohol was also used as a reducing agent with ZVC nanoparticles, but displayed lower degradation efficiency of 70% only. Further, higher oxidation-reduction potential observed for $NaBH_4$ (−1016 mV) in comparison to acidified alcohol (−670 mV) under reaction conditions, confirmed the effectiveness of ZVC-$NaBH_4$ for reductive degradation of chloro-aromatics.

Zeolite supported nano zerovalent iron-copper bimetallic composite (Z-nZVFeCu) synthesized by ion exchange method was used to investigate degradation efficiency of trichloroethylene (TCE) via sodium percarbonate (SPC) activation (Danish et al., 2017). The Z-nZVFeCu acts as a heterogeneous Fenton like catalyst to degrade TCE (> 95%) through the formation of hydroxyl radicals in the system. Higher concentration of hydroxyl radicals were generated using Z-nZVFeCu system as compared to Z-nZVFe (without ZVC) and nZVFe (without zeolite support and ZVC) as analyzed by benzoic acid, a probe indicator used for quantification of ·OH radicals. The enhanced catalytic efficiency of Z-nZVFeCu compared to Z-nZVFe and nZVFe was ascribed to its better stability due to fewer leaching of Cu and Fe from Z-nZVFeCu system, higher surface area of adsorption for rapid diffusion of reactant and product and increased surface active sites resulted from dispersed Fe–Cu bimetallic nanoparticles on the surface of natural zeolite.

### 5.1.2. Phenolic organic pollutants

Phenolic compounds are persistent organic pollutants and due to their long term effect on human health, these are enlisted by the European Union (EU) and United States Environmental Protection Agency (USEPA) as pollutants of priority concern (Mahugo-Santana et al., 2010).

Tetrabromobisphenol A (TBBPA) **8** is the most commonly employed brominated flame retardant (Covaci et al., 2009). However, it is considered as a very harmful contaminant due to its high neurotoxicity, cytotoxicity and immune toxicity associated with its structural features (Lai et al., 2015; Yu et al., 2019). Green rust (GRs) are obtained by partial oxidation of Fe(II) or reduction of Fe(III) salts (Bhave and Shejwalkar, 2018). Green rusts (GRs) interlayered with $Cl^-$, $CO_3^{2-}$, and $SO_4^{2-}$, were effectively used for the dehalogenation of TBBPA (Fang et al., 2019) (Figure 4). However, the zerovalent copper modified green rust with interlayered $Cl^-$ ion exhibits enhanced reductive reactivity for TBBPA. The presence of $CO_3^{2-}$ and $SO_4^{2-}$ has a negative effect on the TBBPA reduction by GR(Cl)–Cu NPs and GR(Cl). The Galvanic cell model was explained for the GR(Cl)–Cu NPs mediated TBBPA reduction, where the electrons were transferred from GR(Cl) to Cu NPs for TBBPA reduction. The reaction intermediates of TBBPA reductive debromination were investigated using LC-MS and were identified as monobromobisphenol A
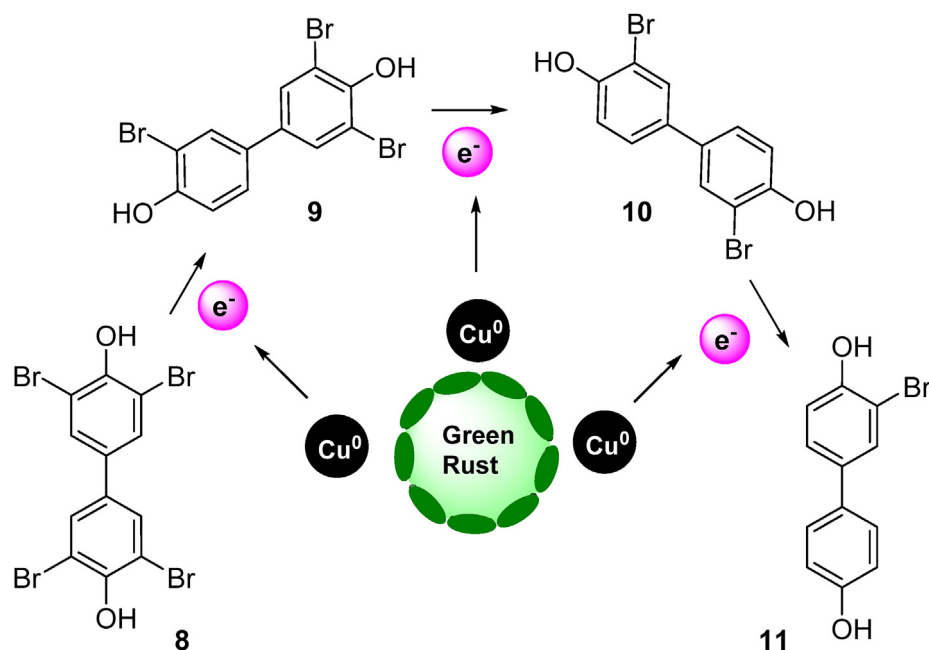
**Figure 4.** Proposed GR(Cl)–Cu NPs mediated reductive debromination pathway for removal of TBBPA **8** (drawn from Fang et al., 2019).

(Mono-BBPA) **11**, dibromobisphenol A (Di-BBPA) **10**, and tribromobisphenol A (Tri-BBPA) **9**.

Nanocomposite ZVC/ZIF-8, a hybrid of zerovalent copper (ZVC) and zeolitic imidazolate framework (ZIF) was obtained by Yang et al. (2019) via immobilizing ZVC (2–8%) onto the surface of ZIF by single-step chemical reduction method. This integrated ZVC/ZIF-8 catalyst exhibits good catalytic efficiency for the p-nitrophenol (PNP) **12** reduction. The complete PNP (0.18 mM) reduction was observed in the presence of $NaBH_4$ (0.17 M) within 2 min of reaction time, using 6%-ZVC/ZIF-8 hybrid (0.003 mg) with highest observed catalytic efficiency and rate constant value of 2.39 $min^{-1}$. In another study, Li et al. (2020) prepared mZn/Cu bimetallic particles by depositing ZVC on surface of Zn and compared it for the p-nitrophenol degradation analysis with other microscale particles like copper on iron (mFe/Cu), metallic iron (mFe), metallic zinc (mZn), metallic copper (mCu), and metallic zinc + metallic copper (mZn + mCu). The removal of total organic carbon (TOC) was observed maximum with mZn/Cu (77%) compared to other systems studied i.e. mZn (5%), mCu/Fe (41%), mCu (19%), mFe (7%), and mZn + mCu (9%). The mZn/Cu system also produced the maximum mineralization, suggesting the oxidative degradation of PNP by ·OH radicals from Fenton-like reactions.

Bisphenol A (2,2-bis(4-hydroxyphenyl)propane, BPA) **14** is an industrial chemical used in the manufacture of epoxy resins and polycarbonate plastics (Abraham and Chakraborty, 2020). However, the BPA is regarded as an endocrine disrupting chemical (Matsushima et al., 2021) and is associated with many adverse effects in humans, including birth defects, development disorders, cancerous tumor, reduced immunity and decreased semen quality etc (Kapustka et al., 2020; Rebai et al., 2021). Organic molecules functionalized ZVC nanoparticles (CuHT, CuPET, and CuPA) synthesized via borohydride reduction of copper(II) nitrate trihydrate salt in the presence of hexanethiol (HT), phenylethanethiol (PET), and phenylacetylene (PA) exhibited significant electro-catalytic activity for oxidation of BPA (Guo et al., 2019). The different pH dependent mechanisms were proposed for BPA oxidation. At pH < 7, ZVC mediated BPA decomposition involves the formation of phenol radical along with isopropyl phenol, which further undergoes one proton oxidation process. However at pH > 7, monohydroxylated BPA formed required two protons for further oxidation. The difference in catalytic efficiencies of *Cu nanoparticle*-modified electrodes was ascribed to outer layer ligands and the proton environment for the BPA oxidation.

In another study performed by Wang et al. (2019b) zerovalent copper mediated activation of persulfate in conjugation with ultrasound radiation was used to investigate bisphenol AF (BPAF) **21** degradation under acidic conditions. The BPAF degradation rate was synergically enhanced from 59.8% to 97.0%, while coupling the heterogeneous Fenton process with the sonolysis. The optimized conditions for the BPAF removal process includes BPAF conc. of 20 mol $L^{-1}$, ZVC conc. of 0.5 $g \cdot L^{-1}$, PS conc. of 1 mM and ultrasound energy of 120 W at 20 kHz (Figure 5).

Duan et al. (2016) investigated the ZVC mediated reductive dechlorination of 4-chlorophenol (4-CP) **20** in aqueous medium and comparison was made with the Cu–Fe bimetallic nanocomposite material. ZVC exhibits higher 4-CP dechlorination efficiency (65%) via direct electron transfer reduction with formation of cyclohexanone as product, whereas the Cu–Fe bimetallic system causes dechlorination via indirect hydrogenation with formation of phenol. The observed dechlorination efficiency of ZVC was a result of conjugation between orbitals of $Cu^0$ and π-orbitals of the benzene of 4-CP. Dechlorination of aliphatic chlorinated compounds such as mono- and dichloroacetic acids was not observed with ZVC due to lack of conjugation.

### 5.1.3. Aromatic amines as pollutants

Aromatic amines are used as source or intermediates in the synthesis of a number of organic compounds of industrial importance such as dyes, drugs, pesticides, fertilizers, cosmetics, polymers, surfactants etc. Due to their carcinogenic nature and bioaccumulations, these are considered an important class of anthropogenic contaminant (Ferraz et al., 2012).

Among the various zero-valent metals ($Fe^0$, $Co^0$, $Al^0$, $Cu^0$) studied for the ozonation degradation of aniline **13**, $Cu^0$ was observed to be the best for the catalytic ozonation activity (Zhang et al., 2017). A significant destruction (98%) of aniline (10 $mg \cdot L^{-1}$) via ozone activation was observed with ZVC (2 $g \cdot L^{-1}$) in a pH range of 4–10 within 24 min of reaction time. EPR analysis confirmed that OH radical was the active species responsible for the aniline degradation, formed from Fenton-like reactions between $Cu^+$ and $H_2O_2$, which were further resulted from a series of redox reactions between ZVC and $O_3$.

Nitroanilines are considered highly toxic and methods/techniques have extensively been developed for their removal or transformation to a less toxic form in the aqueous medium. In one of such approach, Mahmoud et al. (2021) designed a zirconium silicate-nanopolyaniline supported nano zerovalent copper nanocatalyst to perform the catalytic
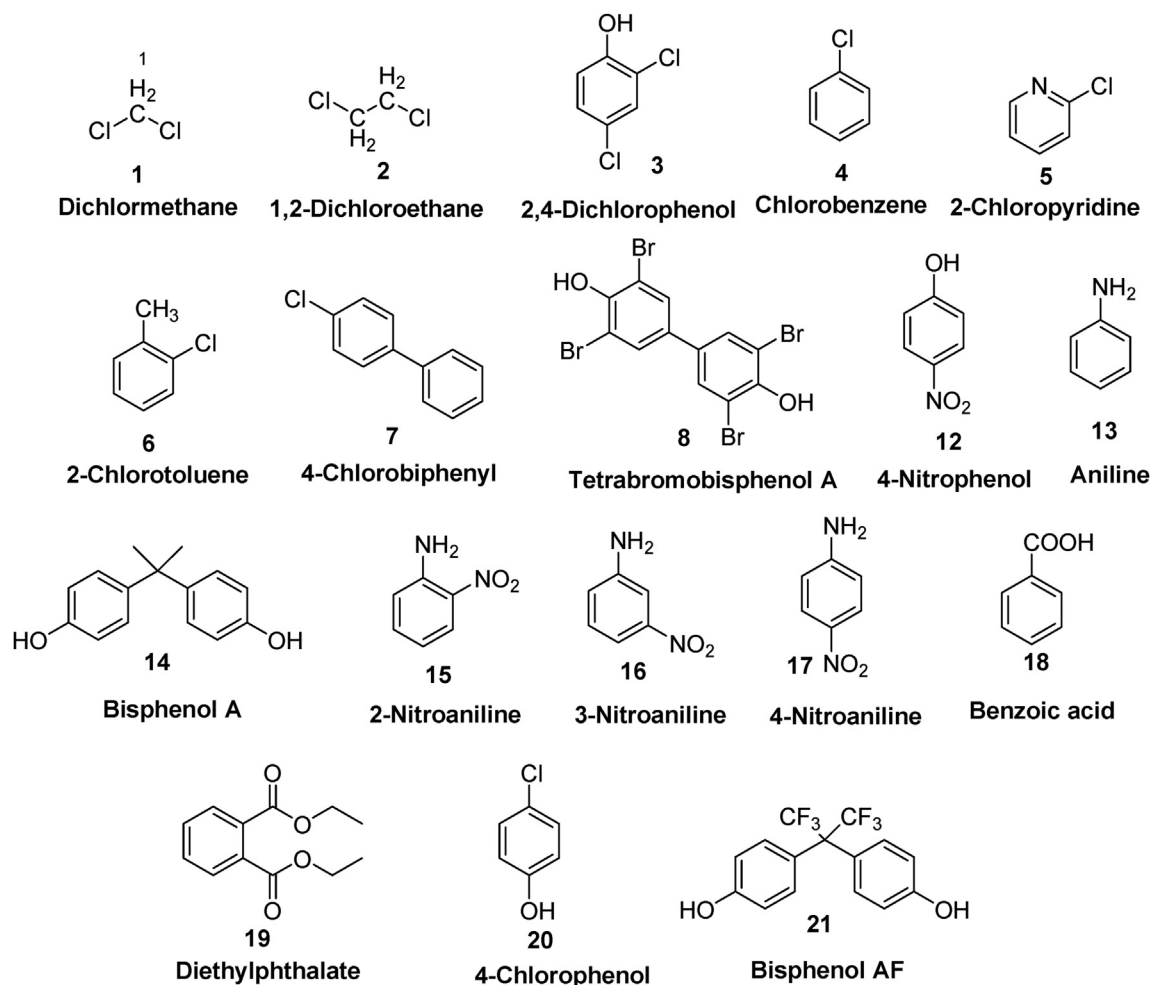
**Figure 5.** Organic molecules studied for the nZVC catalyzed removal processes.

reduction studies of nitroanilines such as 2-nitroaniline **15**, 3-nitroaniline **16**, and 4-nitroaniline **17**. The pseudo-first order kinetics were followed with observed rate constants ($k$) values 0.188, 0.246 and 0.114 min$^{-1}$ for 2-nitroaniline, 3-nitroaniline, and 4-nitroaniline, and the nZVC on the nanocatalyst was considered as the center for the electron transfer process to nitroanilines for the NaBH$_4$ mediated reduction.

### 5.1.4. Aromatic acids and its derivatives as pollutants

Zhou et al. (2016) evaluated the benzoic acid (BA) **18** degradation by using nano-zerovalent copper (nZVC) catalyzed activation of peroxymonosulfate (PMS) under acidic conditions. Complete degradation of BA was achieved with the nZVC/PMS process at initial pH 3 within 10 min of reaction time. Acidic catalyzed release of Cu(I) from ZVC generates hydroxyl radicals ($\cdot$OH) from Fenton like process and sulfate radicals (SO$_4^-$) from PMS activation process were responsible for the increased BA degradation rates. The pseudo-first-order kinetics was observed for the BA degradation, with rate constant value of 0.355 min$^{-1}$.

Wen et al. (2014) performed the oxidative degradation studies of Diethyl phthalate (DEP) **19** using zerovalent copper (ZVC) under oxic conditions. Diethyl phthalate was completely degraded within 2 h of reaction time using 0.5 g·L$^{-1}$ of ZVC at initial pH 2.5. Under acidic conditions, Cu$^+$/Cu$^{2+}$ redox coupled Fenton-like process results in formation of H$_2$O$_2$ from O$_2$, followed by its decomposition to $\cdot$OH radicals was responsible for degradation of DEP, which was further confirmed by inhibition of DEP degradation in the presence of *tert*-butanol, a $\cdot$OH radical scavenger.

Martins et al. (2021) obtained ZVC nanoparticles via recycling process of printed circuit of lead-free computer motherboards and employed as Fenton-like catalyst in the presence of ascorbic acid for the degradation studies of ether amine surfactant used in mining floating.

### 5.2. Removal of dyes

Dyes are another category of organic contaminants which pose a serious threat to sustainable health and the environment due to their non-biocompatible, carcinogenic, and chemically resistant nature. Dyes are excessively produced and used in various industries like tannery (Zhao and Chen, 2019), textiles (Mani and Bharagava, 2016), paints (F D Guerra et al., 2018) and cosmetics (Chaudhary, 2020), etc. These colored compounds not only impart color to the water bodies, but are a threat to aquatic life and life lying higher in the food web including humans (Tkaczyk et al., 2020). In this section, we will discuss the literature reports on the use of zerovalent copper for the removal of dyes (Figure 6) (Table 2).

### 5.2.1. Azo dyes as pollutants

The azo dyes constitute nearly 70% among the commercial dyes used in textile and dye industries around the world (Phugare et al., 2011). Further, it has been estimated that nearly 50% of the total dye content employed for the dyeing process do not bind with the fabric and are released as effluent in industrial wastewater (Rehman et al., 2018). Azo dyes are highly toxic and carcinogenic in nature and prove harmful for aquatic life by increasing the biochemical oxygen demand (BOD) of water (Liu et al., 2017; Phugare et al., 2011). Therefore, there is an utmost need for remediation of these colored harmful contaminants.
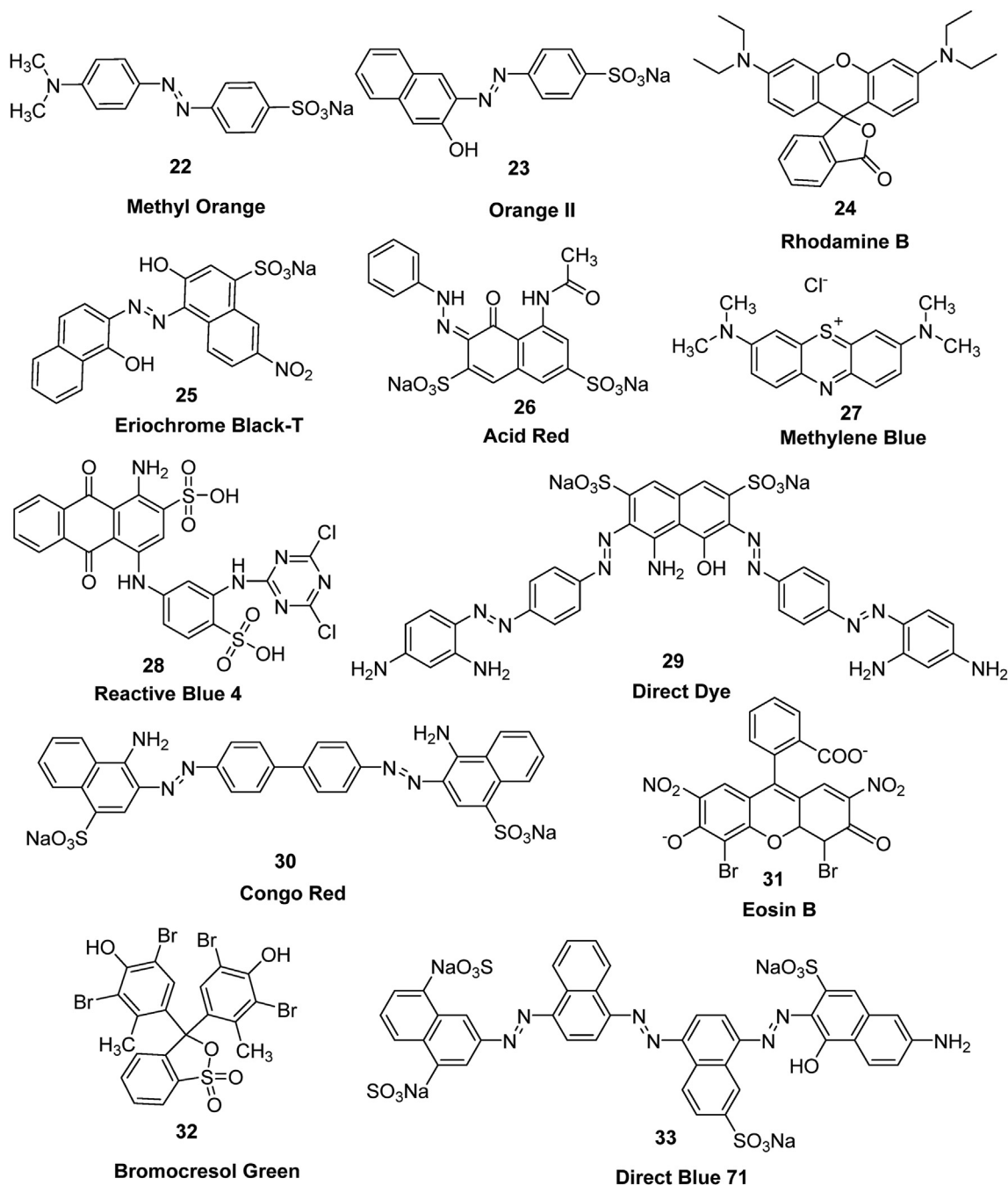
**Figure 6.** Dye molecules studied for the nZVC catalyzed removal process.

Zerovalent copper nanoparticles in the Fenton like process were used for the degradation of methyl orange (MO) azo dye **22** (Li et al., 2015). Hydrodynamic cavitation significantly increased the rate of decolorization of methyl orange by preventing ZVC agglomeration and promoting the generation of hydroxyl radicals in the reaction mixture. Surface adsorption of azo dye onto ZVC was followed by hydrogenation under acidic conditions (pH 3) giving aromatic amines. At the same time, hydroxyl radicals generated from extremely high temperatures resulting from adiabatic compression of cavities causes degradation of dyes. The MO (10 mg·L$^{-1}$) degradation efficiency of 83% was achieved under optimum reaction conditions including ZVC dose of 40 mg·L$^{-1}$, pH 3.0, and 0.4 MPa discharge pressure within 20 min of reaction time. The pseudo first order rate kinetics was observed for the MO degradation, which

increased linearly with the ZVC dose. The reaction intermediates were confirmed from Fourier transform IR (FT-IR) analyses and UV-Vis spectroscopy.

Cu/Fe bimetallic system was prepared by depositing Cu$^0$ on Fe$^0$ surface by a simple metal displacement reaction observed due to a large standard reduction potential difference between Copper and iron i.e. E$_o^r$ is 0.78 V (Yuan et al., 2014). Fe/Cu bimetallic particles exhibits a significant Acid Orange 7 (AO7) **23** removal efficiencies (94.3%) under optimal reaction condition of Cu@Fe conc. of 40 g·L$^{-1}$, AO7 conc. of 1000 mM at initial solution pH of 6.5 within 10 min of reaction time. UV-Vis analysis and FTIR studies confirmed the destruction of chromophore part (-N=N-) that results in formation of 1-amino-2-naphthol and sulfanilamide as degradation intermediates, which are further mineralized during the

**Table 2.** nZVC mediated removal of dyes molecules.

| nZVC (bare or supported) | Pollutant | Oxidizing /Reducing agent (Conc.) | Optimum experimental conditions | | | | Removal (%) | Ref. |
|---|---|---|---|---|---|---|---|---|
| | | | nZVC dose | Pollutant conc. | pH | Time | | |
| Bare | Methyl Orange | - | 40 mg·L$^{-1}$ | 10 mg·L$^{-1}$ | 3 | 20 min. | 3% | (Li et al., 2015) |
| Bare | Congo Red Methyl Orange | NaBH$_4$ (1.25 g.L$^{-1}$) | 1.4 g.L$^{-1}$ | 0.03 mM | - | 5 min. | 90% | (Ismail et al., 2019) |
| Bare | Reactive Blue 4 | - | 1 g.L$^{-1}$ | 15 mg·L$^{-1}$ | 3 | 10 min. | 90% | (Marcelo et al., 2018) |
| TiO$_2$, chitosan, filter paper | Textile dyes | NaBH$_4$ (0.5 g·L$^{-1}$) | - | 0.05 mM | 3 | 5 min. | 98.2% | (Alani et al., 2021) |
| Cellulose filter paper | Congo Red Methyl Orange | NaBH$_4$ (0.26 g·L$^{-1}$) | - | 8.36 mg·L$^{-1}$ 0.98 mg·L$^{-1}$ | - | 13 min. 8 min. | 100% | (Kamal et al., 2016) |
| Carboxymethyl cellulose | Methylene Blue 4-Nitrophenol | NaBH$_4$ (0.26 g·L$^{-1}$) | - | 80 mg·L$^{-1}$ 35 mg·L$^{-1}$ | - | 10.6 h | 100% | (Kamal et al., 2019) |
| Bare | Direct Black | - | 1 g·L$^{-1}$ | 20 mg·L$^{-1}$ | 6.5 | 10 min | 43% | (Ourique et al., 2018) |
| Bare | Eosin B | NaBH$_4$ (0.37 g·L$^{-1}$) | 0.1 mg | 58 mg·L$^{-1}$ | 5 | 0.27 min. | 100% | (Soomro et al., 2014) |
| Bare | Reactive Blue 19 | - | 80 mg·L$^{-1}$ | 0.3 g·L$^{-1}$ | 10 | 75 min | 92.5% | (Haque et al., 2020) |
| Bare | Methyl orange Congo red Methylene blue Rhodamine B | - | 0.3 g·L$^{-1}$ | 20 mg·L$^{-1}$ 20 mg·L$^{-1}$ 10 mg·L$^{-1}$ 5 mg.L$^{-1}$ | 6.6 7.2 7 | 4 h 4 h 168 h 168 h | 56.1% 59.6% 59% 95% | (Dong et al., 2014) |
| Fe(0) | Acid Orange 7 | - | 40 g·L$^{-1}$ | 350 g·L$^{-1}$ | 6.5 | 10 min. | 94.3% | (Yuan et al., 2014) |
| Bare | Orange II | PMS (0.2 g·L$^{-1}$) | 0.3 g·L$^{-1}$ | 8.75 mg·L$^{-1}$ | 3 | 10 min. | 96% | (Liu et al., 2021b) |
| Bare | Direct Blue 71 | H$_2$O$_2$ | 1 g·L$^{-1}$ | 50 mg·L$^{-1}$ | 2.5 | 20 min. | 78% | (Ertugay and Acar, 2013) |
| Carbon nanotube | Congo red | PMS (0.2 g·L$^{-1}$) | 12.7 mg·L$^{-1}$ | 10 mg·L$^{-1}$ | 6.5 | 40 min. | 100% | (Zheng et al., 2021) |

process or are precipitated with Fe ions. In another study performed by Liu et al. (2021b), the ZVC coupled Fe$^{2+}$ ions promoting PMS activation process was used to carry out the degradation of orange II **23** dye. The Cu(III), •OH and SO$_4^{•-}$ was the species identified for the orange II oxidative degradation. Under acidic conditions, ZVC produces Cu$^+$ which reacts with molecular oxygen and produces H$_2$O$_2$. Then both Cu$^+$ and Fe$^{2+}$ induced a Fenton like process to decompose H$_2$O$_2$ and PMS to give ·OH and SO$_4^{•-}$ radicals to cause degradation of orange II dye. Other than orange II dye, the ZVC/Fe(II)/PMS system was able to achieve a degradation efficiency of more than 90% for rhodamine B **24**, methyl orange **22**, acetaminophen **41**, propranolol **49**, ibuprofen **45** and diclofenac **42**.

Ismail et al. (2019) synthesized the stabilized zerovalent copper nanoparticles (CuNPs) using a green process employing the fruit extract of the *Duranta erecta* plant, as evidenced by the emergence of an absorption band at 588 nm in the UV-Vis spectrum. The CuNPs were tested for their efficiency in the reductive degradation of carcinogenic azo dyes such as congo red (CR) **30** and methyl orange **22** using NaBH$_4$, with rate constant values of 5.0710 s$^{-1}$ and 8.610 s$^{-1}$, respectively, based on pseudo-first-order kinetics. In another study, Liu et al. (2016) used visible light to perform zerovalent copper catalyzed photo-degradation of methyl orange dye in aqueous solution. The results obtained from simulation using finite-difference time-domain (FDTD) method suggests that the surface electric charge increases with absorption of light and with decrease in size of nZVC. This results in enhanced photo-catalytic efficiency observed for nZVC for MO degradation.

Zheng et al. (2021) synthesized ZVC supported carbon nanotubes (nZVC–CNT) via simple chemical reduction of pre-adsorbed Cu$^{2+}$ to Cu$^0$ using NaBH$_4$ as a reducing agent. The nZVC–CNT nanocomposite was effectively used as a Fenton-like advanced oxidation process (AOP) via activation of peroxymonosulfate (PMS) to carry degradation of congo red dye **30**. The AOPs system having electrocatalytic membrane was found more effective compared to the conventional batch system. The CNT's carbonyl group (C=O) served as electron donor, while electrophilic oxygen served as electron acceptor to activate PMS to generate hydroxyl radicals (·OH) and singlet oxygen ($^1$O$_2$) to initiate the congo red degradation.

Metallic copper nanoparticles (CuNPs) prepared via reduction route were compared with zinc nanoparticles (ZnNPs) for their degradation efficiency of aqueous Acid Red dye (AR dye) **26**. The CuNPs at its lower

dose (30 mg) were found effective in the degradation of AR dye compared to ZnNPs (80 mg). The experimental data was best fit with a pseudo-second-order kinetic model with higher correlation coefficients. The removal process involves reductive catalytic degradation of AR dye with both CuNPs and ZnNPs. The catalysts were found effective in treatment of real wastewater samples containing AR dye (Salam et al., 2019).

Kamal et al. (2016) loaded zerovalent copper nanoparticles on microfibrous cellulose filter paper coated with chitosan (1%) to give Cu/CH-FP nanocomposite material and investigated for degradation studies of congo red **30** and methyl orange **22** dyes using NaBH$_4$ as reducing agent. The significant rate constant values of 0.1655 and 0.2683 min$^{-1}$ for the CR and MO suggested the good catalytic activity of the composite, which was further complemented with easy removal of dip-like Cu/CH-FP strip from the reaction medium and its reusability with high removal efficiency (75%) even after several cycles. In another studies, carboxymethyl cellulose stabilized nZVCs immobilized on bacterial cellulose nanofiber were synthesized via microwave synthesis and were investigated for their catalytic reduction efficiency of mixed solution of methylene blue **27** and 4-nitrophenol **12** using NaBH$_4$ as reducing agent (Kamal et al., 2019). Although the catalytic performance of bacterial cellulose nanofiber supported nZVC was lower than the carboxymethyl cellulose stabilized nZVC suspension, however, the ease of removal of the supported nZVC make it more convenient to use as heterogeneous catalyst.

Ourique et al. (2018) investigated the degradation efficiencies of ZVC, nZVI and Cu–Fe bimetallic systems towards direct dye from aqueous solutions. The FeNP (100%) and Fe–Cu bimetallic system (90%) were found more effective for the direct dye **29** removal under anoxic conditions compared to ZVC (40%) suggesting the reductive degradation mechanism under conditions studied.

Dong et al. (2014) studied the role of zero-valent copper in activating O$_2$ via electron transfer process at neutral pH to generate different reactive oxygen species (ROS) and release of Cu$^+$ species to participate in Sandmeyer type reaction to break –N=N- bond of azo dyes like methyl orange **22** and congo red **30** to generate carbon centered radicals. The different organic dyes studied were methyl orange **22**, congo red **30**, methylene blue **27** and rhodamine B **24**. The ·OH radicals generated from H$_2$O$_2$ destruction then reacted with carbon centered radicals causing
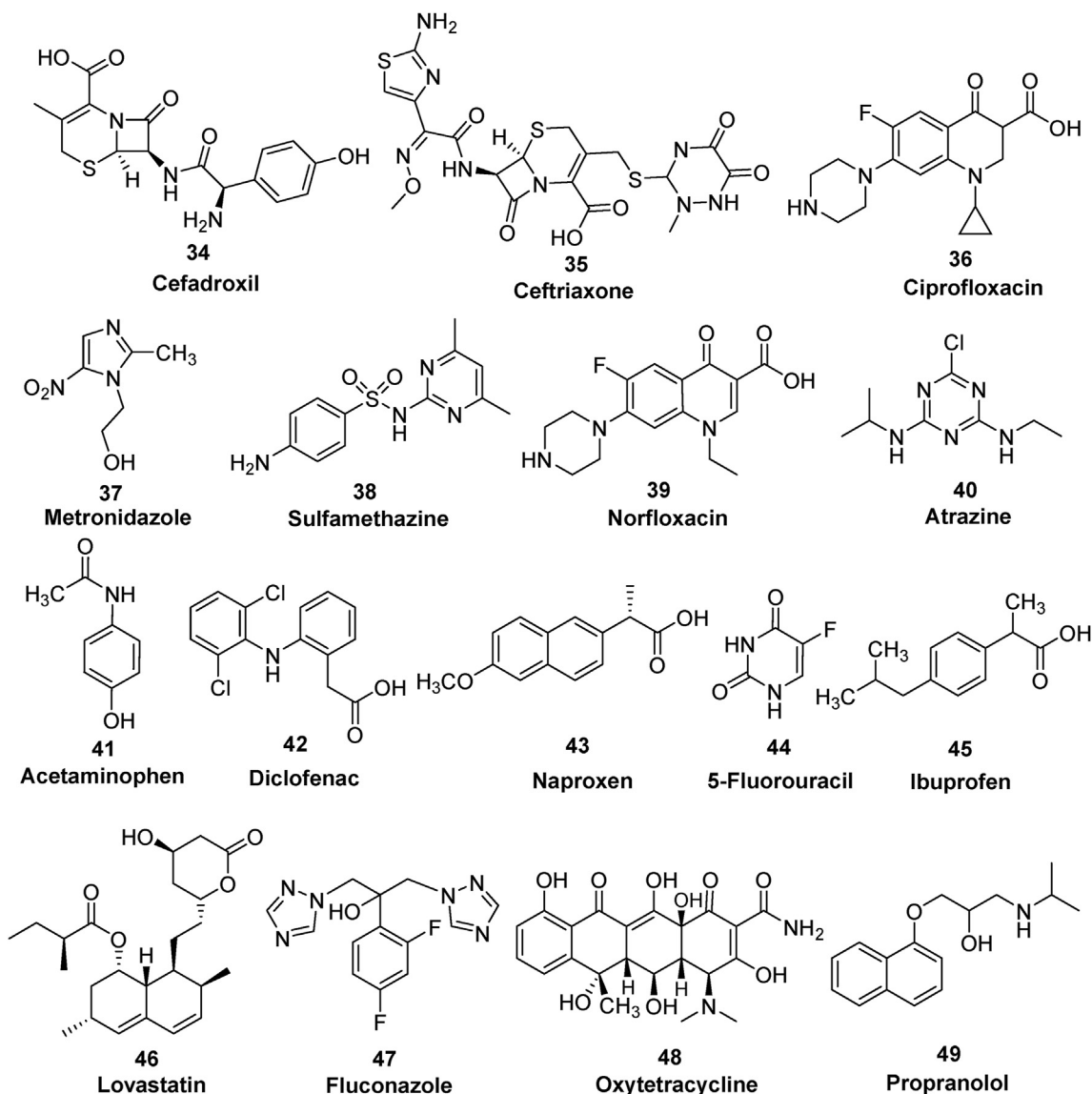
**Figure 7.** Pharmaceuticals studied for the nZVC catalyzed removal process.

transformation of organic compounds to low molecular weight acids with subsequent mineralization. GCMS technique confirmed the presence of different degradation fragments resulting from carbon centered radical destruction processes of different azo dyes. ESR confirmed the presence of ˙OH and O$_2^-$ radical species in the reaction conditions.

Ertugay et al. (2013) performed the ZVC mediated sonocatalytic degradation of Direct Blue 71 (DB71) **33** under acidic conditions at 20 kHz with ultrasound power of 95W. Approximately 55.8% dye (50 mg·L$^{-1}$) removal was achieved under optimum reaction conditions of 1 g·L$^{-1}$ of catalyst at initial pH of 2.5 at 20 °C within the reaction time of 20 min. The dye removal efficiency was further increased to 78% in the presence of H$_2$O$_2$ as an oxidizing agent under reaction conditions.

### 5.2.2. Anthraquinone dyes as pollutant

After azo dyes, the anthraquinone based dye molecules are the second largest organic dye compounds produced worldwide for coloring of textile fabrics. Owing to their complex and reinforced structure, the anthraquinone based dyes provide a natural resistance to degradation process and thus pose a serious threat to the environment (Routoula et al., 2020).

Zero-valent copper nanoparticles (nZVC) were also investigated for the removal of the Reactive Blue 4 dye (Marcelo et al., 2018). Approx.

90% of the oxidative degradation with concomitant mineralization of RB4 dye was achieved within the 10 min of reaction time as confirmed from Total Organic Carbon (TOC) analysis. Cu(I) mediated oxidative process was responsible for the removal process instead of ˙OH radicals as confirmed from the use of tert-Butyl alcohol as ˙OH captor. The reaction rate was decreased with increase in initial concentration of dye and increased with decrease in pH (from 7 to 3), increase in temperature (from 10 to 30 °C) and increase in nZVC dose (from 0.5 to 2 g·L$^{-1}$). Experimental data was best fit using a second-order kinetics model and activation energy determined was 42 kJ mol$^{-1}$. The nZVC nanoparticles exhibit good recyclability without any significant loss of RB4 removal efficiencies. A greener approach involving the use of fish scales of *Labeo rohita* was employed for the synthesis of zerovalent copper and later was applied for the decolorization reaction of Reactive Blue 19 dye **28** (Haque et al., 2020).

### 5.2.3. Fluorescein dyes as pollutant

Fluorescein dyes are used as fluorescent tracers and have many applications in biological systems. These are considered non-toxic, non-pollutant and non-carcinogenic, however, there release in water system increases the biochemical oxygen demands (BOD). Alani et al. (2021) synthesized the zero-valent copper nanoparticles immobilized onto a

**Table 3.** nZVC mediated removal of drug molecules.

| nZVC (bare or supported) | Pollutant | Oxidizing /Reducing agent (Conc.) | Optimum experimental conditions | | | | Removal (%) | Ref. |
|---|---|---|---|---|---|---|---|---|
| | | | nZVC dose | Pollutant conc. | pH | Time | | |
| Bare | Cefadroxil Ceftriaxone | - | 1 $gL^{-1}$ | 76 $mgL^{-1}$ 50 $mgL^{-1}$ | 9.5 | 20 min. | 85% 97% | (Oliveira et al., 2018) |
| Bare | Ciprofloxacin | - | 0.5 $gL^{-1}$ | 20 $mgL^{-1}$ | 3.5 | 2h | 100% | (de Sousa et al., 2019) |
| Graphene | Metronidazole | - | 0.5 $gL^{-1}$ | 20 $mgL^{-1}$ | 3.2 | 20 min. | 92% | (Xu et al., 2019) |
| Bare | Acetaminophen | - | 5 $gL^{-1}$ | 50 $mgL^{-1}$ | 3 | 4h | 100% | (Zhang et al., 2017b) |
| Bare | Norfloxacin | $H_2O_2$ (0.68 $gL^{-1}$) | 0.25 $gL^{-1}$ | 5 $mgL^{-1}$ | - | 30 min. | 92% | (Ma et al., 2018) |
| Bare | Norfloxacin | PS (0.22 $gL^{-1}$) | 0.05 $gL^{-1}$ | 10 $mgL^{-1}$ | - | 5 min. | 100% | (Deng et al., 2019) |
| Bare | Sulfamethazine | PS (0.11 $gL^{-1}$) | 64 $mgL^{-1}$ | 5 $mgL^{-1}$ | 3.06 | 60 min. | 100% | (Zhang et al., 2020b) |
| Montmorillonite | Atrazine | - | 0.5 $gL^{-1}$ | 12.5 $mgL^{-1}$ | 3.0 | 2 min. | 90% | (Hong et al., 2017) |
| Bare | Acetaminophen | PMS (0.2 $gL^{-1}$) | 0.5 $gL^{-1}$ | 7.5 $mgL^{-1}$ | 3.0 | 12 min. | 89% | (Liu et al., 2021a) |
| Bare | Diclofenac | PAA (7.6 $gL^{-1}$) | 0.5 $gL^{-1}$ | 0.30 $mgL^{-1}$ | 3.0 | 40 min. | 95.5% | (Zhang et al., 2021) |
| Graphene | Naproxen | PMS (0.3$gL^{-1}$) | 2 $gL^{-1}$ | 1.15 $mgL^{-1}$ | 3.0 | 30 min. | 91% | (Chi et al., 2019) |
| Bare | 5-Fluorouracil Lovastatin | - | 25 $mgL^{-1}$ | 50 $mgL^{-1}$ | 6.8 | 90 min. | 65.1% 78.19% | (Dinesh et al., 2020) |
| Vanadium-doped | Fluconazole | $H_2O_2$ (1.7 $gL^{-1}$) | 1 $gL^{-1}$ | 20 $mgL^{-1}$ | 3 | 60 min. | 100% | (Zhang et al., 2020a) |
| $Fe_3O_4$ | Oxytetracycline | $H_2O_2$ (0.6 $gL^{-1}$) | 1 $gL^{-1}$ | 20 $mgL^{-1}$ | 3 | 10 min. | 97% | (Kim and Ko, 2018) |

porous support consisting of $TiO_2$, Chitosan and filter paper to produce nanocomposite material (Cu/CHTiO$_2$/FP). The nanocomposite has pronounced catalytic efficiency for textile dyes like rhodamine B **24**, methyl orange **22**, eriochrome black-T **25** and bromocresol green **32** using $NaBH_4$ as a reducing agent. It's easy recovery and reusability with high dye removal efficiency (> 90%) even after five cycles make it an efficient material for remediation of colored compounds.

Soomro et al. (2014) studied the sodium dodecyl sulfate (SDS) capped ZVC for reductive degradation of Eosin B (EB) dye **31**. Approximately 100 % removal efficiency of EB (100 µM) was achieved within a reaction time of 20 s using 500 µL of $NaBH_4$ (10 mM) and 0.1 mg ZVC catalyst. The enhanced catalytic activity of nanocatalyst was a result of rough surface evident from AFM analysis, providing a greater number of active sites for reaction.

In another study performed by Ghanbari et al. (2014) the sulfate radicals generated by zerovalent iron and copper mediated activation of peroxymonosulfate was used for the decoloration of textile wastewater. ZVI was found to be more effective for TOC and COD removal when compared to ZVC. However, among the ZVC mediated activation of PMS and $H_2O_2$ for the decoloration of textile wastewater, the former was proved more significant. Further, the simultaneous employment of PMS and $H_2O_2$, synergically enhanced the decoloration efficiencies of both ZVC and ZVI.

### 5.3. Removal of drugs

Pharmaceutical products or drugs are another category of organic contaminants, which enter the ecosystem through different pathways extending from pharmaceutical industrial disposal to metabolites of human healthcare medicines. Due to their persistent nature, they may prove harmful to aquatic life and also to humans. This part of the discussion will present literature reports employing zerovalent copper used for the removal of pharmaceutical products (Figure 7) (Table 3).

Oliveira et al. (2018) studied the nZVC for the removal of cefadroxil **34** and ceftriaxone **35** antibiotics from aqueous solution under oxic and anoxic conditions. More than 85% of the antibiotics were removed within a reaction time of 20 min. Use of tert-butyl alcohol as a radical inhibitor confirmed that the hydroxyl radicals is not the sole requirement of the antibiotic degradations, but the presence of Cu$^+$ was responsible for the overall removal process. Two-step removal process was observed, whereby the Cu$^+$ species promoted degradation of antibiotics was deliberated as the first step followed by adsorption of antibodies on the copper oxides/hydroxides in the second step. Both these removal steps followed pseudo first order kinetic models. Nearly 57% of

cefadroxil removal was obtained within 180 min as observed from TOC analysis.

In another study, degradation of ciprofloxacin **36** by metallic copper nanoparticles was investigated under aqueous conditions (de Sousa et al., 2019b). The optimum conditions involve 20 $mgL^{-1}$ ciprofloxacin concentrations, 0.5 $gL^{-1}$ nZVC dose with solution pH of 3.5. Under acidic conditions, Cu(I) mediated formation of active oxygen radicals were responsible for the degradation of ciprofloxacin. However, adsorption and coprecipitation were observed as primary phenomena for the removal of antibiotics under the basic conditions, which was further confirmed from the desorption experiments. Increase in dose concentration, temperature and chloride anions favors the degradation kinetics, whereas increase in sulfate anion concentration has inhibitory effect on the ciprofloxacin degradations. A reduction in reusable efficiency (70% removal) was observed due to surface passivation of nZVC nanoparticles due to formation of $Cu_2O$ in consecutive cycles.

A self-assembly involving the liquid-phase reduction process was used for the synthesis of 3D-macroporous graphene-wrapped nZVC nanocomposite (3D-GN@Cu$^0$). The composite material displayed high efficiencies for the degradation of aqueous metronidazole **37** saturated with dissolved oxygen under various pH conditions ranging from 3.2 to 9.8, without using $H_2O_2$ as oxidizing agent (Xu et al., 2019). Activation of dissolved oxygen to surface bounded ·OH via Fenton-like process was observed from the XPS analysis of the sample and held responsible for the degradative removal of metronidazole. The DFT calculation was used to justify the results obtained from micro-electrolysis of 3D-GN@Cu$^0$ and also explained the observed synergistic effect between graphene and nZVCs for the removal of metronidazole.

Zhang et al. (2020b) performed sulfamethazine (SMZ) **38** degradations using a synergistic approach involving nZVC and sonolysis promoted activation of persulfate to give $SO_4^{•-}$. The optimal conditions for the complete SMZ removal includes a PS dose of 0.5 mM, nZVC conc. of 64 $mgL^{-1}$, reaction time of 60 min, ultrasound energy of 0.4 W/mL and 40 kHz at solution pH of 3.06. The inhibitory effect was observed with anions like sulfate, nitrate, bicarbonate and chloride ions. The major degradation pathways proposed includes S–N bond cleavage, $SO_2$ extrusion (Smile rearrangement), and oxidative degradation of aniline moiety.

Degradation analysis of norfloxacin (NOR) **39**, a fluoroquinolone based antibiotic was performed by Deng et al. (2019) using nZVC/PS system with application of mild temperature (40 °C). The temperature enhanced the release of Cu$^+$ from nZVC in the solution promoting the formation of ·OH and $SO_4^{•-}$ species responsible for degradation of norfloxacin. In another study, Ma et al. (2018) used a synergistic effect
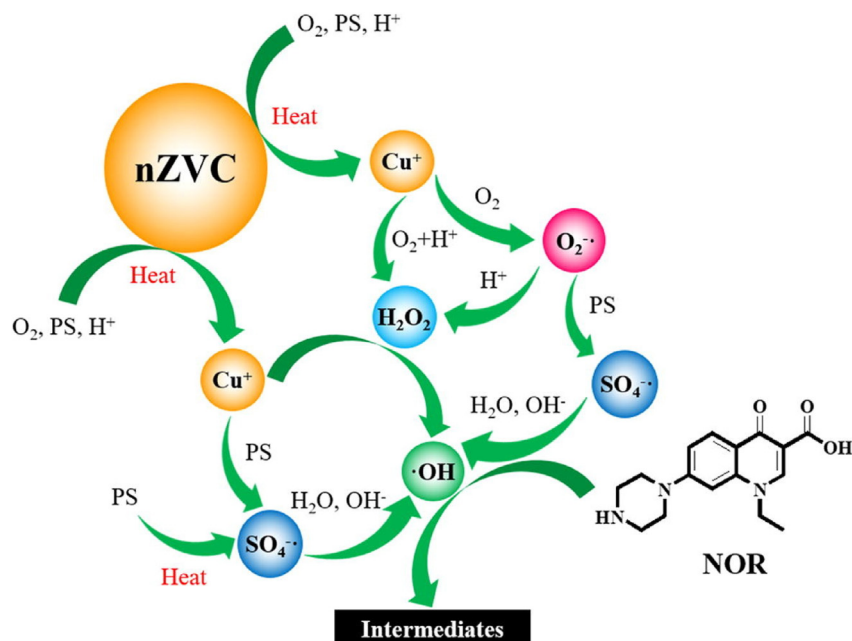
**Figure 8.** nZVC mediated activation of persulfate and degradation of norfloxacin (Deng et al., 2019).

between ZVC and ultrasonic irradiation (US) to activate $H_2O_2$ to induce a Fenton-like reaction. Nearly 100% degradation was observed within 30 min. of the reaction time using 0.25 $g \cdot L^{-1}$ of nZVC, 10 mM conc. of $H_2O_2$ with US of 240 W at 20 kHz. EPR analysis confirmed the presence of $\cdot OH$ radicals as the primary species responsible for NOR degradation and superoxide radicals ($O_2^-$) as a mediator for regeneration of $Cu^+$ from oxidized form of copper i.e. $Cu^{2+}$. The oxidative cleavage of piperazine

moiety and transformation of quinolone was regarded as a major degradation step among other reported oxidation pathways (Figure 8).

Hong et al. (2017) evaluated the montmorillonite clay supported zerovalent copper (ZVCMMT) for the degradation analysis of atrazine **40**. The montmorillonite supported ZVC exhibited a significant atrazine removal efficiency (90%) compared to conventionally prepared ZVCs. Further the hydration status of prepared nanocomposite strongly
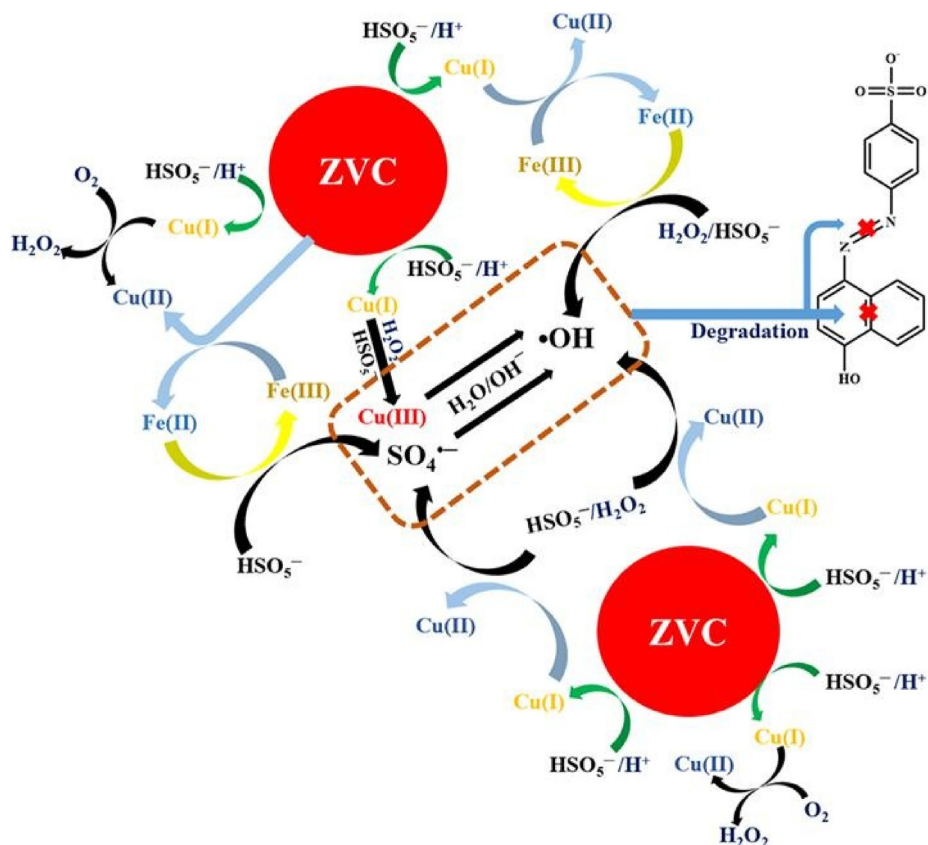


**Figure 9.** Schematic representation of acetaminophen removal by Fe(III)/Cu(0)/PMS system (Liu et al., 2021a).
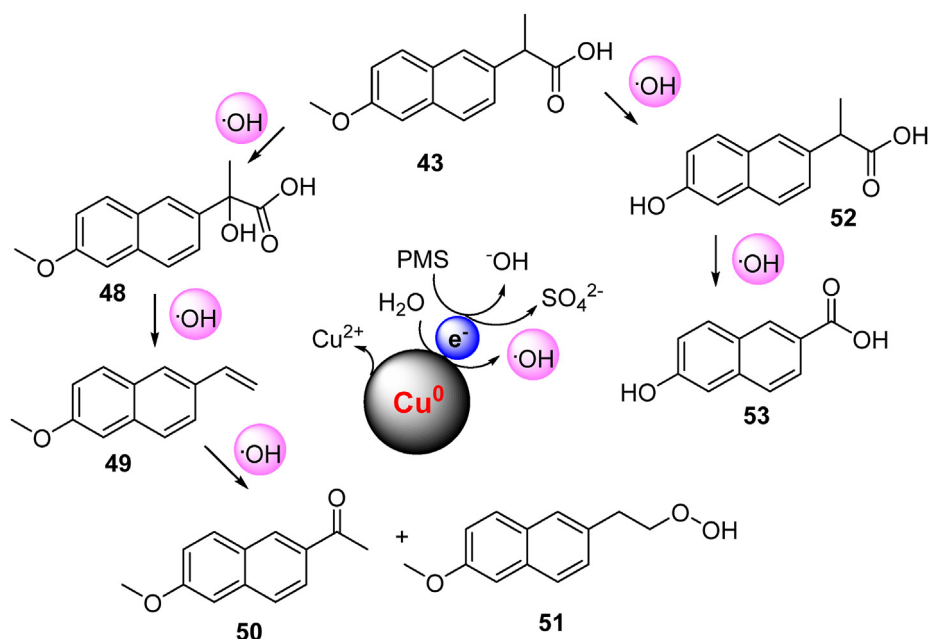
**Figure 10.** Proposed pathways for naproxen **43** degradation in ZVC-PMS activation system (redrawn from Chi et al., 2019).

determines the atrazine degradation efficiency by controlling the adsorption of oxygen and atrazine residues on the freeze dried surface of the nanocomposite. The prepared ZVCMMT nanocomposite significantly decreased the toxicity of atrazine in the studied reaction conditions.

Zhang et al. (2017b) used commercially synthesized ZVC for the investigation of acetaminophen (ACT) **41** degradation by *in-situ* generated reactive oxygen species (ROS) like $H_2O_2$, hydroxyl radical ($\cdot OH$) and superoxide anion radical ($O_2^{\cdot-}$) under acidic conditions (pH 3). The $Cu^+$ ion generated from ZVC under acidic conditions not only produces $H_2O_2$ via activation of $O_2$, but also helped in its decomposition to produce $\cdot OH$ species, actually involved in the degradation process of acetaminophen and further confirmed by ESR analysis. The superoxide anion radical ($O_2^{\cdot-}$)

helped in the regeneration of $Cu^+$ from its oxidized forms i.e. $Cu^{2+}$ via one electron transfer process. In another study performed by Liu et al. (2021a) the $Fe^{3+}$ addition to the ZVC/PMS significantly enhanced the acetaminophen degradation. ZVC promotes PMS oxidation under acidic conditions by single electron transfer resulting in formation of $Cu^+$. The $Fe^{3+}$ interacts with both $Cu^+$ and $Cu^0$ to generate $Fe^{2+}$, which is considered more active compared to $Cu^+$ in generation of $\cdot OH$ radicals from the Fenton-like process. In the final step, both $Cu^+$ and $Fe^{2+}$ activate $H_2O_2$ and PMS for the acetaminophen degradation (Figure 9). Common ions in water including sulfate, carbonate, and nitrate had no adverse effect on acetaminophen degradation process by Fe(III)/ZVC/PMS system, whereas humic acid and chloride ions slightly inhibit the acetaminophen degradation process.
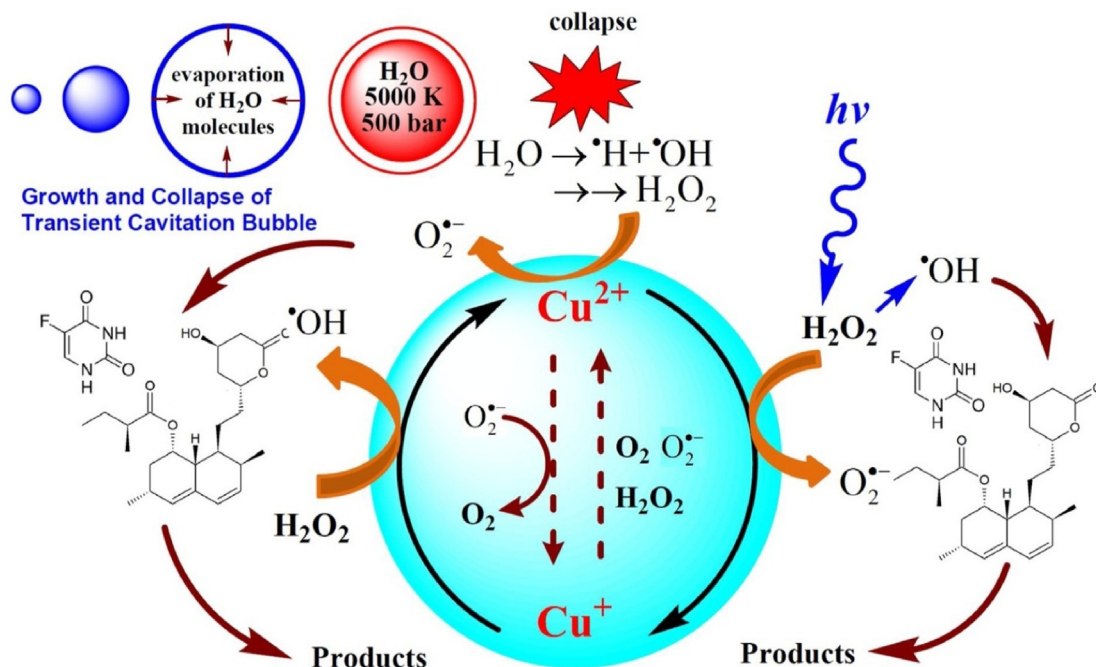


**Figure 11.** Ultrasound assisted degradation mechanism of Lovastatin **46** and 5-Fluorouracil **44** drug molecules in the presence of nZVC (Dinesh et al., 2020).

**Table 4.** nZVC mediated removal of heavy metals.

| nZVC (bare or supported) | Pollutant | Optimum experimental conditions | | | | Removal (%) | Ref. |
|---|---|---|---|---|---|---|---|
| | | nZVC dose | Pollutant conc. | pH | Time | | |
| Chitosan | Chromium | 1 g·L$^{-1}$ | 50 mg·L$^{-1}$ | 2.85 | 5 h | 47.8 | (Wu et al., 2009) |
| Bare | Uranium | 0.03 g·L$^{-1}$ | 0.1 mg·L$^{-1}$ | 4 | 1 h | 130 | (Chandra and Khan, 2020) |
| Biochar | Lead | 2.5 g·L$^{-1}$ | 70 mg·L$^{-1}$ | 7 | 12 h | 29.57 | (Din et al., 2021) |
| Pistachio shell powder | Chromium | 0.1 g·L$^{-1}$ | 20 mg·L$^{-1}$ | 3 | 17 h | 93.5 | (Kumar et al., 2021) |

Zhang et al. (2021) used zerovalent copper for the activation of peracetic acid to give radical species like $\cdot$OH, $CH_3COO\cdot$ and $CH_3COOO\cdot$ to study the degradation profile of sodium salt of diclofenac **42**. Corrosion of ZVC to $Cu^+$ species at pH 3 was responsible for the activation of peracetic acid, hydrogen peroxide and molecular oxygen. UPLC-QTOF/MS analysis suggested seven different degradation pathways depending on the detection of six different degradation products as: (i) hydroxylation; (ii) amidation; (iii) dechlorination-cyclizaiton; (iv) dechlorination-hydrogenation; (v) dechlorination-hydroxylation; (vi) decarboxylation; and (vii) formylation.

Chi et al. (2019) employed the ZVC-activated PMS system for the evaluation of the degradation mechanism of naproxen **43**, an anti-inflammatory drug. Four different forms of ZVC have been employed for the PMS activation namely copper sheet, copper foam, graphene-copper sheet, and graphene-copper foam. ZVC coating with graphene results in an increase in naproxen degradation efficiency by 10% and decrease in $Cu^{2+}$ release by 30%. ESR analysis and radical scavenging studies confirmed that hydroxyl radicals were the dominant species responsible for degradation other than sulfate radicals. On the basis of HPLC-MS/MS analysis, six different intermediates were identified and thus helped in proposing the naproxen degradation pathway (Figure 10).

The *Hibiscus Rosa-Sinensis* extract as a reducing as well as stabilizing agent for the synthesis of ZVC nanoparticles (Dinesh et al., 2020). The ultrasound energy helped in controlling the crystallinity and size of the ZVC nanoparticles during the synthesis process. The synthesized ZVC displayed amphoteric nature with dual catalyst activation mechanism in the presence of UVC-light or ultrasound irradiation. The ZVC nanoparticles displayed high degradation efficiencies of 91.3% and 93.2% for 5-fluorouracil **44** and lovastatin **46** drugs, respectively. The hydroxyl radicals generated from UV irradiation combined with the sonolysis process and oxidation of $Cu^+$ to $Cu^{2+}$ during ultrasound irradiation were responsible for degradation of drugs. The degradation process was further enhanced by superoxide radical ($O_2^-$) produced from reaction of in-situ generated $H_2O_2$ with $Cu^{2+}$ (Figure 11).

Zhang et al. (2020a) investigated the removal efficiencies of Cu–V bimetallic catalyst, prepared via hydrothermal approach, towards fluconazole **47** an active antifungal pharmaceutical product. Addition of vanadium to copper material not only improved its surface properties like number electron-rich center around active sites, surface defects and adsorption capacities that result into enhancement of catalytic efficiencies of bimetallic system, but also helped in decreasing $Cu^{2+}$ concentrations by reducing it back to give active $Cu^+$ species. The surface oxygen vacancies helped in easy destruction of *in-situ* generated $H_2O_2$ via Fenton-system to give $\cdot$OH radicals responsible for the oxidative degradation of fluconazole. The EPR analysis and radical scavenging test further confirmed the involvement of $\cdot$OH radicals.

A *core*-shell structure based $Cu@Fe_3O_4$ nanocomposite consisting of ZVC as core and $Fe_3O_4$ as protective shell was synthesized by Kim et al. (2018) using a simple reduction method. $Cu@Fe_3O_4$ displayed exceptional synergistic effect in oxidative degradation of oxytetracycline **48**, an antibiotic used in personal care products via a Fenton-like reaction. More than 99% oxytetracycline (20 mg·L$^{-1}$) degradation was achieved within 10 min of the reaction time using 1 g·L$^{-1}$ dose of $Cu@Fe_3O_4$, 20mM conc. of $H_2O_2$ at pH 3 and pH 9.

## 5.4. Removal of heavy metals

Heavy metals are considered highly toxic due to their high degree of bioaccumulation efficiencies (Bonsignore et al., 2018; Vajargah, 2021) and the role it plays in the inhibition of various enzymatic activities in humans that result in organ damage (Fu and Xi, 2020; Lopina, 2017). Although the reports are limited, zerovalent copper has been effectively used for the remediation of heavy metals from aqueous medium (Table 4).

Chitosan-tripolyphosphate containing chelating resin beads was used as a support for the synthesis of copper-chitosan composite material, in which the copper (II) ions were first adsorbed on to the surface of chitosan-tripolyphosphate beads followed by reduction using chemical process that results into well dispersed copper nanoparticles on the surface of chitosan beads (Wu et al., 2009). The prepared copper-chitosan composite material was compared with the chitosan-tripolyphosphate beads for their removal efficiencies of aqueous hexavalent chromium via adsorption, co-precipitation or redox mechanisms, and was found to have better adsorption efficiencies than later. The optimum conditions to obtain maximum adsorption of Cr(VI) involves copper-chitosan nanocomposite dose of 1 g·L$^{-1}$ and Cr(VI) initial concentration of 50 mg·L$^{-1}$ at pH 2.85. From EDS analysis it was evident that the adsorption of Cr(VI) was observed both on the surface (10.53 wt.%) as well as the inside (5.13 wt.%) of the copper-chitosan nanocomposite.

Uranium concentration in water if exceeds its permissible limits proves carcinogenic for humans and other living beings. *Nano zerovalent* copper synthesized by environment-friendly green method using testa extract of *Anacardium occidentale* was evaluated for the removal of uranium from aqueous solution (Chandra and Khan, 2020). Polyphenolic functional groups present in the *Anacardium occidentale* testa extract not only reduce the Cu(II) to Cu(0), but also act as stabilizing agent for the synthesized nZVCs. The maximum adsorption efficiency (96.63%) was achieved with nZVC dose of 0.03 g·L$^{-1}$ for 100 ppb initial concentration of uranium with a reaction time of 60 min. at pH 4. The best fit of experimental data was obtained using Langmuir adsorption isotherm ($R_L$ = 0.1733) and Freundlich adsorption isotherm ($R^2$ = 0.99) models.

Din et al. (2021) used cotton stalk biochar as a support to synthesize zerovalent copper nanocomposite materials and tested for its adsorption abilities to remove lead from the aqueous solutions. Kinetic equilibrium studies suggest the pseudo-second-order to be followed with rate constant value of 720 min. for lead removal by ZVC composite. Study of thermodynamic parameters points towards the spontaneous but endothermic chemisorptive nature of the adsorption process.

Kumar et al. (2021) prepared the pistachio shell supported zerovalent copper (nZVC @PS) and studied its synergistic effect for the removal of Cr(VI) from the aqueous solutions using the adsorption efficiency of pistachio shell powder and reduction capacities of zerovalent copper (Figure 12). The nanocomposite exhibits significant Cr(VI) removal efficiencies (110.9 mg·g$^{-1}$), when compared to other nanocomposite reports.

Overall, it may be concluded that the best removal efficiencies for nZVC towards various environment pollutants can be achieved under acidic pH 3–6, regardless of the target contaminant. However, the progressive explanations may vary in different contaminant removal studies, but the enhanced dissolution and formation of Cu$^I$ species from Cu$^0$ is

**Figure 12.** Schematic illustration of Cr(VI) removal by nZVC@PS using synergistic effect (Kumar et al., 2021).

regarded as a conclusive hypothesis for the generation of reactive oxygen species responsible for the degradation of organic contaminants under acidic conditions. The contaminant removal efficiencies of nZVC were observed to be increased with increase in dose of nZVC, concentration of oxidizing or reducing agent and application of external energy source, with a significant decrease in reaction time. The novelty of the review article in this study includes the summarization of research results of the various nZVC mediated contaminant degradation studies in tabulated form to provide an opportunity for the researchers to understand the optimum experimental parameter and conditions involved in the pollutant removal process.

## 6. Conclusion and future perspectives

*Nanoscale zerovalent* copper (nZVC) has proved expedient in solving many of the problems related to the existence of organic/inorganic contaminants in the environment and their adverse effects on the ecosystem. Owing to their small size, high surface area, stability associated with their core-shell structure, tendency to degrade organic contaminants under oxic/anoxic conditions either by generation of various reactive oxygen species like $H_2O_2$, $O_2^-$, $\cdot OH$ etc. under given reaction conditions, or by reductive removal of contaminants via single or double electron transfer processes made them a suitable candidate for the various studies involving environment remediation processes. However, their stability and activity to control various oxidative/reductive processes largely depends on their storage conditions and surface passivation. The contaminant removal process by nZVC is a pH controlled process, mostly observed in the pH range 3–6, which may be attributed to dissolution of surface oxide layer, conversion of $Cu^0$ to $Cu^I$ and generation of reactive oxygen species via Fenton-like process under acidic conditions. Alkaline pH results in formation of surface mixed oxide layer and facilitates the contaminant removal process by surface adsorption. The research focused on evaluating the various optimum experimental parameters and conditions to achieve the maximum contaminant

removal efficiency from nZVC mediated degradation process. The research also evaluated the role of copper species involved in the catalytic generation of radical species responsible for degradation, and effect of presence of oxidizing and reducing agents.

Further, various materials of synthetic or biogenic origin used as immobilizers or supports may not only provide the stability to the synthesized nano zerovalent copper particles but also significantly alter their physical and chemical properties. Although various supports has been used for the synthesis of nZVC@support based nanocomposite materials, however, the effect of immobilizer on the adsorption and redox properties of nZVC or the origin of synergistic effect when the two worked together for the removal of contaminants has been less studied. In this context, there are significant possibilities to perform research in this field to determine the various activating and stabilizing factors that an immobilizer provides to the synthesized nZVC particles and the underlying mechanism for the contaminant removal via synergistic effect.

## Declarations

### *Author contribution statement*

All authors listed have significantly contributed to the development and the writing of this article.

### *Funding statement*

### *Data availability statement*

Data included in article/supplementary material/referenced in article.

## Declaration of interests statement

The authors declare no conflict of interest.

## Additional information

No additional information is available for this paper.

## Acknowledgements

## References

Abboud, Y., Saffaj, T., Chagraoui, A., El Bouari, A., Brouzi, K., Tanane, O., Ihssane, B., 2014. Biosynthesis, characterization and antimicrobial activity of copper oxide nanoparticles (CONPs) produced using brown alga extract (*Bifurcaria bifurcata*). Appl. Nanosci. 4, 571–576.

Abhiman, G., Devi, P.S., Vijayalakshmi, K., 2018. Green synthesis with antibacterial investigation of Copper nanoparticles using *Azadirachta indica* (neem) leaf extract. Themed Section: Sci. Technol. 4, 697–701.

Abraham, A., Chakraborty, P., 2020. A review on sources and health impacts of bisphenol A. Rev. Environ. Health 35, 201–210.

Ahmedova, A., Todorov, B., Burdzhiev, N., Goze, C., 2018. Copper radiopharmaceuticals for theranostic applications. Eur. J. Med. Chem. 157, 1406–1425.

Akhtar, F.Z., Archana, K., Krishnaswamy, V.G., Rajagopal, R., 2020. Remediation of heavy metals (Cr, Zn) using physical, chemical and biological methods: a novel approach. SN Appl. Sci. 2, 1–14.

Alani, O.A., Ari, H.A., Offiong, N.-A.O., Alani, S.O., Li, B., Zeng, Q-r, Feng, W., 2021. Catalytic removal of selected textile dyes using zero-valent copper nanoparticles loaded on filter paper-chitosan-titanium oxide heterogeneous support. J. Polym. Environ. 1–15.

Ali, N., Kamal, T., Ul-Islam, M., Khan, A., Shah, S.J., Zada, A., 2018. Chitosan-coated cotton cloth supported copper nanoparticles for toxic dye reduction. Int. J. Biol. Macromol. 111, 832–838.

Alymov, M., Rubtsov, N., Seplyarskii, B., Zelenskii, V., Ankudinov, A., Tsvetkov, G., Chernysh, V., 2018. Effect of Production Conditions on the Size of Copper Nanoparticles and the Modes of Ignition and Combustion of a Copper Nanopowder in Air, Doklady Chemistry. Springer, pp. 318–322.

Amer, M.W., Awwad, A.M., 2021. Green synthesis of copper nanoparticles by Citrus limon fruits extract, characterization and antibacterial activity. Chem. Int. 7, 1–8.

Andal, V., Buvaneswari, G., 2017. Effect of reducing agents in the conversion of Cu$_2$O nanocolloid to Cu nanocolloid. Eng. Sci. Tech. Int. J. 20, 340–344.

Arya, A., Gupta, K., Chundawat, T.S., Vaya, D., 2018. Biogenic synthesis of copper and silver nanoparticles using green alga *Botryococcus braunii* and its antimicrobial activity. Bioinorganic Chemistry and Applications.

Asghar, M.A., Asghar, M.A., 2020. Green synthesized and characterized copper nanoparticles using various new plants extracts aggrave microbial cell membrane damage after interaction with lipopolysaccharide. Int. J. Biol. Macromol. 160, 1168–1176.

Balasubramanian, P., Velmurugan, M., Chen, S.-M., Hwa, K.-Y., 2017. Optimized electrochemical synthesis of copper nanoparticles decorated with reduced graphene oxide: application for enzymeless determination of glucose in human blood. J. Electroanal. Chem. 807, 128–136.

Begletsova, N., Selifonova, E., Chumakov, A., Al-Alwani, A., Zakharevich, A., Chernova, E., Glukhovskoy, E., 2018. Chemical synthesis of copper nanoparticles in aqueous solutions in the presence of anionic surfactant sodium dodecyl sulfate. Colloids Surf. A Physicochem. Eng. Asp. 552, 75–80.

Behera, M., Giri, G., 2014. Green synthesis and characterization of cuprous oxide nanoparticles in presence of a bio-surfactant. Materials Science-Poland 32, 702–708.

Berman, R., Macdonald, D.K.C., 1952. The thermal and electrical conductivity of copper at low temperatures. Proc. Roy. Soc. Lond. Math. Phys. Sci. 211, 122–128.

Beverskog, B., Puigdomenech, I., 1997. Revised Pourbaix diagrams for copper at 25 to 300 °C. J. Electrochem. Soc. 144, 3476–3483.

Bhave, C., Shejwalkar, S., 2018. A review on the synthesis and applications of green rust for environmental pollutant remediation. Int. J. Environ. Sci. Technol. 15, 1243–1248.

Bonsignore, M., Manta, D.S., Mirto, S., Quinci, E.M., Ape, F., Montalto, V., Gristina, M., Traina, A., Sprovieri, M., 2018. Bioaccumulation of heavy metals in fish, crustaceans, molluscs and echinoderms from the Tuscany coast. Ecotoxicol. Environ. Saf. 162, 554–562.

Chandra, C., Khan, F., 2020. Nano-scale zerovalent copper: green synthesis, characterization and efficient removal of uranium. J. Radioanal. Nucl. Chem. 324, 589–597.

Chang, P.-H., Chou, T.-H., Sahu, R.S., Shih, Y-h, 2019. Chemical reduction-aided zerovalent copper nanoparticles for 2, 4-dichlorophenol removal. Appl. Nanosci. 9, 387–395.

Chaudhary, B., 2020. Chemistry of synthetic dyes: a review. J. Interdiscip. Cycle Res. 12, 390–396.

Chen, H., Lee, J.H., Kim, Y.H., Shin, D.W., Park, S.C., Meng, X., Yoo, J.B., 2010. Metallic copper nanostructures synthesized by a facile hydrothermal method. J. Nanosci. Nanotechnol. 10, 629–636.

Chen, C., Peters, J.C., Fu, G.C., 2021. Photoinduced copper-catalysed asymmetric amidation via ligand cooperativity. Nature 596, 250–256.

Chi, H., Wang, Z., He, X., Zhang, J., Wang, D., Ma, J., 2019. Activation of peroxymonosulfate system by copper-based catalyst for degradation of naproxen: mechanisms and pathways. Chemosphere 228, 54–64.

Chung, I.M., Abdul Rahuman, A., Marimuthu, S., Vishnu Kirthi, A., Anbarasan, K., Padmini, P., Rajakumar, G., 2017. Green synthesis of copper nanoparticles using Eclipta prostrata leaves extract and their antioxidant and cytotoxic activities. Exp. Ther. Med. 14, 18–24.

Covaci, A., Voorspoels, S., Abdallah, M.A.-E., Geens, T., Harrad, S., Law, R.J., 2009. Analytical and environmental aspects of the flame retardant tetrabromobisphenol-A and its derivatives. J. Chromatogr. A 1216, 346–363.

Dadras, M., Morris, D.G., 1997. Examination of some high-strength, high-conductivity copper alloys for high-temperature applications. Scripta materialia 38.

Daehn, K., Allanore, A., 2020. Electrolytic production of copper from chalcopyrite. Current Opin. Electrochem. 22, 110–119.

Danish, M., Gu, X., Lu, S., Ahmad, A., Naqvi, M., Farooq, U., Zhang, X., Fu, X., Miao, Z., Xue, Y., 2017. Efficient transformation of trichloroethylene activated through sodium percarbonate using heterogeneous zeolite supported nano zero valent iron-copper bimetallic composite. Chem. Eng. J. 308, 396–407.

Dash, P., Balto, Y., 2011. Generation of nano-copper particles through wire explosion method and its characterization. Res. J. Nanosci. Nanotechn. 1, 25–33.

Davis, J.R., 2001. Copper and Copper Alloys. ASM international.

Deng, J., Xu, M., Chen, Y., Li, J., Qiu, C., Li, X., Zhou, S., 2019. Highly-efficient removal of norfloxacin with nanoscale zero-valent copper activated persulfate at mild temperature. Chem. Eng. J. 15, 491–503.

de Sousa, P.V.F., de Oliveira, A.F., da Silva, A.A., Lopes, R.P., 2019a. Environmental remediation processes by zero valence copper: reaction mechanisms. Environ. Sci. Pollut. Control Ser. 26, 14883–14903.

de Sousa, P.V.F., de Oliveira, A.F., da Silva, A.A., Vaz, B.G., Lopes, R.P., 2019b. Study of ciprofloxacin degradation by zero-valent copper nanoparticles. Chem. Pap. 73, 249–260.

Din, M.I., Rehan, R., 2017. Synthesis, characterization, and applications of copper nanoparticles. Anal. Lett. 50, 50–62.

Din, S.U., Awan, J.M., Imran, M., Haq, S., Hafeez, M., Hussain, S., Khan, M.S., 2021. Novel. Nanocomposite of biochar-zerovalent copper for lead adsorption. Microscopy Research and Technique.

Dinesh, G.K., Pramod, M., Chakma, S., 2020. Sonochemical synthesis of amphoteric Cu0-Nanoparticles using Hibiscus rosa-sinensis extract and their applications for degradation of 5-fluorouracil and lovastatin drugs. J. Hazard Mater. 399, 123035.

Dong, G., Ai, Z., Zhang, L., 2014. Total aerobic destruction of azo contaminants with nanoscale zero-valent copper at neutral pH: promotion effect of in-situ generated carbon center radicals. Water Res. 66, 22–30.

Dong, J., Ye, J., Ariyanti, D., Wang, Y., Wei, S., Gao, W., 2018. Enhancing photocatalytic activities of titanium dioxide via well-dispersed copper nanoparticles. Chemosphere 204, 193–201.

Dong, X.-Y., Zhang, Y.-F., Ma, C.-L., Gu, Q.-S., Wang, F.-L., Li, Z.-L., Jiang, S.-P., Liu, X.-Y., 2019. A general asymmetric copper-catalysed Sonogashira C (sp 3)–C (sp) coupling. Nat. Chem. 11, 1158–1166.

Doong, R.-A., Chen, K.T., Tsai, H.C., 2003. Reductive dechlorination of carbon tetrachloride and tetrachloroethylene by zerovalent silicon-iron reductants. Environ. Sci. Technol. 37, 2575–2581.

Dror, I., Fink, L., Weiner, L., Berkowitz, B., 2020. Elucidating the catalytic degradation of enrofloxacin by copper oxide nanoparticles through the identification of the reactive oxygen species. Chemosphere 258, 127266.

Duan, J., Zhu, H., Xu, F., Zhao, J., 2016. A new approach to 4-chlorophenol dechlorination on monometallic copper compared to its Cu/Fe bimetallic system. Chem. Eng. J. 304, 282–288.

El-Saadony, M.T., El-Hack, A., Mohamed, E., Taha, A.E., Fouda, M.M., Ajarem, J.S., N Maodaa, S., Allam, A.A., Elshaer, N., 2020. Ecofriendly synthesis and insecticidal application of copper nanoparticles against the storage pest Tribolium castaneum. Nanomaterials 10, 587.

Endo, K., 2002. Synthesis and structure of poly (vinyl chloride). Prog. Polym. Sci. 27, 2021–2054.

Ertugay, N., Acar, F., 2013. Removal of direct blue 71 By heterogeneous sono, photo and sonophotocatalytic oxidation: zero valent copper catalyst. J. Selcuk Univ. Nat. Appli. Sci. 580–593.

Essa, H.L., Abdelfattah, M.S., Marzouk, A.S., Shedeed, Z., Guirguis, H.A., El-Sayed, M.M., 2021. Biogenic copper nanoparticles from Avicennia marina leaves: impact on seed germination, detoxification enzymes, chlorophyll content and uptake by wheat seedlings. PLoS One 16, e0249764.

Fang, L., Liu, R., Xu, L., Li, J., Huang, L.-Z., Li, F., 2019. Enhanced debromination of tetrabromobisphoenol a by zero-valent copper-nanoparticle-modified green rusts. Environ. Sci. J. Integr. Environ. Res.: Nano 6, 970–980.

Fang, Y., Guo, Y., 2018. Copper-based non-precious metal heterogeneous catalysts for environmental remediation. Chin. J. Catal. 39, 566–582.

Fathima, J.B., Pugazhendhi, A., Oves, M., Venis, R., 2018. Synthesis of eco-friendly copper nanoparticles for augmentation of catalytic degradation of organic dyes. J. Mol. Liq. 260, 1–8.

Feng, J., Lim, T.T., 2005. Pathways and kinetics of carbon tetrachloride and chloroform reductions by nano-scale Fe and Fe/Ni particles: comparison with commercial micro-scale Fe and Zn. Chemosphere 59, 1267–1277.

Feng, J., Chen, D., Sediq, A.S., Romeijn, S., Tichelaar, F.D., Jiskoot, W., Yang, J., Koper, M.T., 2018. Cathodic corrosion of a bulk wire to nonaggregated functional nanocrystals and nanoalloys. ACS Appl. Mater. Interfaces 10, 9532–9540.

Ferraz, E.R., de Oliveira, G.A., de Oliveira, D.P., 2012. The impact of aromatic amines on the environment: risks and damages. Front. Biosci. 4, 914–923.

Fu, Z., Xi, S., 2020. The effects of heavy metals on human metabolism. Toxicol. Mech. Methods 30, 167–176.

Gao, Y., Wu, T., Yang, C., Ma, C., Zhao, Z., Wu, Z., Cao, S., Geng, W., Wang, Y., Yao, Y., 2021. Activity trends and mechanisms in peroxymonosulfate-assisted catalytic production of singlet oxygen over atomic metal-N-C catalysts. Angew. Chem. Int. Ed. 60, 22513–22521.

Gawande, M.B., Goswami, A., Felpin, F.-X., Asefa, T., Huang, X., Silva, R., Zou, X., Zboril, R., Varma, R.S., 2016. Cu and Cu-based nanoparticles: synthesis and applications in catalysis. Chem. Rev. 116, 3722–3811.

Ghanbari, F., Moradi, M., Manshouri, M., 2014. Textile wastewater decolorization by zero valent iron activated peroxymonosulfate: compared with zero valent copper. J. Environ. Chem. Eng. 2, 1846–1851.

Goncharova, D.A., Kharlamova, T.S., Lapin, I.N., Svetlichnyi, V.A., 2019. Chemical and morphological evolution of copper nanoparticles obtained by pulsed laser ablation in liquid. J. Phys. Chem. C 123, 21731–21742.

Guerra, E., Llompart, M., Garcia-Jares, C., 2018. Analysis of dyes in cosmetics: challenges and recent developments. Cosmetics 5, 47.

Guerra, F.D., Attia, M.F., Whitehead, D.C., Alexis, F., 2018. Nanotechnology for environmental remediation: materials and applications. Molecules 23, 1760.

Guo, Y., Sun, Y., Wang, Y., He, H., Zhu, Y., 2019. Thiol-and alkyne-functionalized copper nanoparticles as electrocatalysts for bisphenol A (BPA) oxidation. J. Solid State Electrochem. 23, 91–100.

Gutierrez, J.A., Silber, J.J., Falcone, R.D., Correa, N.M., 2021. Modified reverse micelle method as facile way to obtain several gold nanoparticle morphologies. J. Mol. Liq. 331, 115709.

Haque, A., Kiran, S., Nosheen, S., Afzal, G., Gulzar, T., Ahmad, S., Rehman, S., Tariq, M.H., 2020. Degradation of reactive blue 19 dye using copper nanoparticles synthesized from Labeo rohita fish scales: a greener approach. Pol. J. Environ. Stud. 29, 609–616.

Hashimi, A.S., Ginting, R.T., Chin, S.X., Lau, K.S., Nohan, M.A.N.M., Zakaria, S., Yap, C.C., Chia, C.H., 2020. Fast microwave-assisted synthesis of copper nanowires as reusable high-performance transparent conductive electrode. Curr. Appl. Phys. 20, 205–211.

Honary, S., Barabadi, H., Gharaei-Fathabad, E., Naghibi, F., 2012. Green synthesis of copper oxide nanoparticles using Penicillium aurantiogriseum, Penicillium citrinum and Penicillium waksmanii. Dig. J. Nanomater. Bios. 7, 999–1005.

Hong, R., Guo, Z., Gao, J., Gu, C., 2017. Rapid degradation of atrazine by hydroxyl radical induced from montmorillonite templated subnano-sized zero-valent copper. Chemosphere 180, 335–342.

Huang, C.-C., Lo, S.-L., Lien, H.-L., 2012. Zero-valent copper nanoparticles for effective dechlorination of dichloromethane using sodium borohydride as a reductant. Chem. Eng. J. 203, 95–100.

Huang, C.-C., Lo, S.-L., Lien, H.-L., 2013. Synergistic effect of zero-valent copper nanoparticles on dichloromethane degradation by vitamin B12 under reducing condition. Chem. Eng. J. 219, 311–318.

Huang, C.-C., Lo, S.-L., Tsai, S.-M., Lien, H.-L., 2011. Catalytic hydrodechlorination of 1, 2-dichloroethane using copper nanoparticles under reduction conditions of sodium borohydride. J. Environ. Monit. 13, 2406–2412.

Huang, Y., Liu, Z., Gao, G., Xiao, G., Du, A., Bottle, S., Sarina, S., Zhu, H., 2017. Stable copper nanoparticle photocatalysts for selective epoxidation of alkenes with visible light. ACS Catal. 7, 4975–4985.

Ismail, M., Gul, S., Khan, M., Khan, M.A., Asiri, A.M., Khan, S.B., 2019. Green synthesis of zerovalent copper nanoparticles for efficient reduction of toxic azo dyes Congo red and methyl orange. Green Process. Synth. 8, 135–143.

Issaabadi, Z., Nasrollahzadeh, M., Sajadi, S.M., 2017. Green synthesis of the copper nanoparticles supported on bentonite and investigation of its catalytic activity. J. Clean. Prod. 142, 3584–3591.

Kamal, T., Ahmad, I., Khan, S.B., Ul-Islam, M., Asiri, A.M., 2019. Microwave assisted synthesis and carboxymethyl cellulose stabilized copper nanoparticles on bacterial cellulose nanofibers support for pollutants degradation. J. Polym. Environ. 27, 2867–2877.

Kamal, T., Khan, S.B., Asiri, A.M., 2016. Synthesis of zero-valent Cu nanoparticles in the chitosan coating layer on cellulose microfibers: evaluation of azo dyes catalytic reduction. Cellulose 23, 1911–1923.

Kapoor, S., Mukherjee, T., 2003. Photochemical formation of copper nanoparticles in poly (N-vinylpyrrolidone). Chem. Phys. Lett. 370, 83–87.

Kapustka, K., Ziegmann, G., Klimecka-Tatar, D., Ostrega, M., 2020. Identification of health risks from harmful chemical agents-review concerning bisphenol A in workplace. Prod. Eng. Archives 26.

Khodashenas, B., Ghorbani, H.R., 2014. Synthesis of copper nanoparticles : an overview of the various methods. Kor. J. Chem. Eng. 31, 1105–1109.

Kim, D.-G., Ko, S.-O., 2018. Oxidative degradation of the antibiotic oxytetracycline by Cu@ Fe3O4 core-shell nanoparticles. Sci. Total Environ. 631, 608–618.

Kim, I., Kim, Y., Woo, K., Ryu, E.-H., Yon, K.-Y., Cao, G., Moon, J., 2013. Synthesis of oxidation-resistant core–shell copper nanoparticles. RSC Adv. 3, 15169–15177.

Kim, S., Kim, J.H., Kwon, W.Y., Hwang, S.H., Cha, B.S., Kim, J.M., Oh, S.S., Park, K.S., 2019. Synthesis of DNA-templated copper nanoparticles with enhanced fluorescence stability for cellular imaging. Microchim. Acta 186, 1–5.

Kumar, S., Brar, R.S., Babu, J.N., Dahiya, A., Saha, S., Kumar, A., 2021. Synergistic effect of pistachio shell powder and nano-zerovalent copper for chromium remediation from aqueous solution. Environ. Sci. Pollut. Control Ser. 28, 63422–63436.

Kumar, B.R., Etika, K.C., 2022. Facile one-pot hydrothermal synthesis of copper nanowires and their impact on the EMI shielding capability of epoxy composites. Chem. Eng. Technol. 45, 410–416.

Lai, D., Liu, T., Jiang, G., Chen, W., 2013. Synthesis of highly stable dispersions of copper nanoparticles using sodium hypophosphite. J. Appl. Polym. Sci. 128, 1443–1449.

Lai, D.Y., Kacew, S., Dekant, W., 2015. Tetrabromobisphenol A (TBBPA): possible modes of action of toxicity and carcinogenicity in rodents. Food Chem. Toxicol. 80, 206–214.

Lamichhane, J.R., Osdaghi, E., Behlau, F., Köhl, J., Jones, J.B., Aubertot, J.-N., 2018. Thirteen Decades of Antimicrobial Copper Compounds Applied in Agriculture. A Review, 38. Agronomy for Sustainable Development, pp. 1–18.

Lee, C.-L., Jou, C.-J.G., Huang, H., 2010. Degradation of chlorobenzene in water using nanoscale Cu coupled with microwave irradiation. J. Environ. Eng. 136, 412–416.

Lee, H.J., Song, J.Y., Kim, B.S., 2013. Biological synthesis of copper nanoparticles using Magnolia kobus leaf extract and their antibacterial activity. J. Chem. Technol. Biotechnol. 88, 1971–1977.

Li, N., Liang, J., Wei, D., Zhu, Y., Qian, Y., 2014. Solvothermal synthesis of micro-/ nanoscale Cu/Li4Ti5O12 composites for high rate Li-ion batteries. Electrochim. Acta 123, 346–352.

Li, L., Hu, J., Shi, X., Fan, M., Luo, J., Wei, X., 2016. Nanoscale zero-valent metals: a review of synthesis, characterization, and applications to environmental remediation. Environ. Sci. Pollut. Control Ser. 23, 17880–17900.

Li, P., Song, Y., Wang, S., Tao, Z., Yu, S., Liu, Y., 2015. Enhanced decolorization of methyl orange using zero-valent copper nanoparticles under assistance of hydrodynamic cavitation. Ultrason. Sonochem. 22, 132–138.

Li, W., Fan, X., Liu, B., Zhang, Y., Zhou, L., Lan, Y., 2020. Synthesis of microscale zinc–copper bimetallic particles and their performance toward p-nitrophenol removal: characterization, mineralization, and response surface methodology. Environ. Eng. Sci. 37, 263–271.

Liang, Y., Lin, F., Adeli, Y., Jin, R., Jiao, N., 2019. Efficient electrocatalysis for the preparation of (hetero) aryl chlorides and vinyl chloride with 1, 2-dichloroethane. Angew. Chem. Int. Ed. 58, 4566–4570.

Lin, C.J., Lo, S.-L., Liou, Y.H., 2005. Degradation of aqueous carbon tetrachloride by nanoscale zerovalent copper on a cation resin. Chemosphere 59, 1299–1307.

Liu, C., Dong, H., Ji, Y., Rujisamphan, N., Li, Y., 2019. High-performance hydrogen evolution reaction catalysis achieved by small core-shell copper nanoparticles. J. Colloid Interface Sci. 551, 130–137.

Liú, D., Wang, G., Liü, D., Lin, J., He, Y., Li, X., Li, Z., 2016. Photocatalysis using zero-valent nano-copper for degrading methyl orange under visible light irradiation. Opt. Mater. 53, 155–159.

Liu, J., Dhungana, B., Cobb, G.P., 2018. Environmental behavior, potential phytotoxicity, and accumulation of copper oxide nanoparticles and arsenic in rice plants. Environ. Toxicol. Chem. 37, 11–20.

Liu, Q-m, Zhou, D-b, Yamamoto, Y., Ichino, R., Okido, M., 2012. Preparation of Cu nanoparticles with NaBH4 by aqueous reduction method. Trans. Nonferrous Metals Soc. China 22, 117–123.

Liu, N., Xie, X., Yang, B., Zhang, Q., Yu, C., Zheng, X., Xu, L., Li, R., Liu, J., 2017. Performance and microbial community structures of hydrolysis acidification process treating azo and anthraquinone dyes in different stages. Environ. Sci. Pollut. Control Ser. 24, 252–263.

Liu, X., Xu, P., Fu, Q., Li, R., He, C., Yao, W., Wang, L., Xie, S., Xie, Z., He, Q., 2021a. Ferric ion promoted degradation of acetaminophen with zero− valent copper activated peroxymonosulfate process. Chem. Eng. J. 426, 131679.

Liu, X., Xu, P., Fu, Q., Li, R., He, C., Yao, W., Wang, L., Xie, S., Xie, Z., Ma, J., 2021b. Strong degradation of orange II by activation of peroxymonosulfate using combination of ferrous ion and zero-valent copper. Separ. Purif. Technol. 278, 119509.

Lopina, O.D., 2017. Enzyme inhibitors and activators, enzyme inhibitors and activators. IntechOpen.

Lu, L., Shen, Y., Chen, X., Qian, L., Lu, K., 2004. Ultrahigh strength and high electrical conductivity in copper. Science 304, 422–426.

Ma, X., Cheng, Y., Ge, Y., Wu, H., Li, Q., Gao, N., Deng, J., 2018. Ultrasound-enhanced nanosized zero-valent copper activation of hydrogen peroxide for the degradation of norfloxacin. Ultrason. Sonochem. 40, 763–772.

Mahmoud, M.E., Amira, M.F., Seleim, S.M., Abouelanwar, M.E., 2021. Behavior of surface coated zirconium silicate-nanopolyaniline with nano zerovalent copper (ZrSiO4@ NPANI@nZVCu) toward catalytic reduction of nitroanilines. Mater. Chem. Phys. 258, 123890.

Mahmoud, S.H., Gan, T.Y., 2018. Impact of anthropogenic climate change and human activities on environment and ecosystem services in arid regions. Sci. Total Environ. 633, 1329–1344.

Mahugo-Santana, C., Sosa-Ferrera, Z., Torres-Padrón, M.E., Santana-Rodríguez, J.J., 2010. Analytical methodologies for the determination of nitroimidazole residues in biological and environmental liquid samples: a review. Anal. Chim. Acta 665, 113–122.

Majumder, D., 2012. Bioremediation: copper nanoparticles from electronic-waste. Int. J. Eng. Sci. Technol. 4.

Maki, K., Ito, Y., Matsunaga, H., Mori, H., 2013. Solid-solution copper alloys with high strength and high electrical conductivity. Scripta Mater. 68, 777–780.

Mallick, S., Sabui, P., 2021. Green synthesis of copper and copper-based nanoparticles for their use in medicine: toxicity and safety. Nanotech. Med.: Toxic. Safety 174–194.

Mani, S., Bharagava, R.N., 2016. Exposure to crystal violet, its toxic, genotoxic and carcinogenic effects on environment and its degradation and detoxification for environmental safety. Rev. Environ. Contam. Toxicol. 237 237, 71–104.

Marcelo, C.R., Puiatti, G.A., Nascimento, M.A., Oliveira, A.F., Lopes, R.P., 2018. Degradation of the reactive blue 4 dye in aqueous solution using zero-valent copper nanoparticles. J. Nanomater.

Martins, T.A.G., Falconi, I.B.A., Pavoski, G., de Moraes, V.T., Baltazar, M. d P.G., Espinosa, D.C.R., 2021. Green synthesis, characterization, and application of copper nanoparticles obtained from printed circuit boards to degrade mining surfactant by Fenton process. J. Environ. Chem. Eng. 9, 106576.

Matavos-Aramyan, S., Moussavi, M., 2017. Advances in Fenton and Fenton based oxidation processes for industrial effluent contaminants control - a review. Int. J. Environ. Sci. Na. Resource 2, 555594.

Matsushima, A., Teramoto, T., Kakuta, Y., 2021. Crystal structure of endocrine-disrupting chemical bisphenol A and estrogen-related receptor γ. J. Biochem.

Mdlovu, N.V., Chiang, C.-L., Lin, K.-S., Jeng, R.-C., 2018. Recycling copper nanoparticles from printed circuit board waste etchants via a microemulsion process. J. Clean. Prod. 185, 781–796.

Minneci, R.P., Lass, E.A., Bunn, J.R., Choo, H., Rawn, C.J., 2021. Copper-based alloys for structural high-heat-flux applications: a review of development, properties, and performance of Cu-rich Cu–Cr–Nb alloys. Int. Mater. Rev. 66, 394–425.

Moskalyk, R., Alfantazi, A., 2003. Review of copper pyrometallurgical practice: today and tomorrow. Miner. Eng. 16, 893–919.

Murai, K., Watanabe, Y., Saito, Y., Nakayama, T., Suematsu, H., Jiang, W., Yatsui, K., Shim, K., Niihara, K., 2007. Preparation of copper nanoparticles with an organic coating by a pulsed wire discharge method. J. Ceram. Process. Res. 8, 114.

Nagar, N., Devra, V., 2018. Green synthesis and characterization of copper nanoparticles using Azadirachta indica leaves. Mater. Chem. Phys. 213, 44–51.

Nasrollahzadeh, M., Sajadi, S.M., 2015. Green synthesis of copper nanoparticles using Ginkgo biloba L. leaf extract and their catalytic activity for the Huisgen [3+ 2] cycloaddition of azides and alkynes at room temperature. J. Colloid Interface Sci. 457, 141–147.

Noor, S., Shah, Z., Javed, A., Ali, A., Hussain, S.B., Zafar, S., Ali, H., Muhammad, S.A., 2020. A fungal based synthesis method for copper nanoparticles with the determination of anticancer, antidiabetic and antibacterial activities. J. Microbiol. Methods 174, 105966.

Numaga, N., Hayashi, H., Smith, R.L., 2020. Supercritical hydrothermal synthesis of polyacrylic acid-capped copper nanoparticles and their feasibility as conductive nanoinks. J. Electron. Mater. 49, 5681–5686.

Ojha, N.K., Zyryanov, G.V., Majee, A., Charushin, V.N., Chupakhin, O.N., Santra, S., 2017. Copper nanoparticles as inexpensive and efficient catalyst: a valuable contribution in organic synthesis. Coord. Chem. Rev. 353, 1–57.

Oliveira, L.M., Nascimento, M.A., Guimarães, Y.M., Oliveira, A.F., Silva, A.A., Lopes, R.P., 2018. Removal of beta-lactams antibiotics through zero-valent copper nanoparticles. J. Braz. Chem. Soc. 29, 1630–1637.

Ourique, M.F., Sousa, P.V., Oliveira, A.F., Lopes, R.P., 2018. Comparative study of the direct black removal by Fe, Cu, and Fe/Cu nanoparticles. Environ. Sci. Pollut. Control Ser. 25, 28928–28941.

Padma, P.N., Banu, S.T., Kumari, S.C., 2018. Studies on green synthesis of copper nanoparticles using Punica granatum. Annual Res. Rev. Bio. 1–10.

Panagos, P., Ballabio, C., Lugato, E., Jones, A., Borrelli, P., Scarpa, S., Orgiazzi, A., Montanarella, L., 2018. Potential sources of anthropogenic copper inputs to European agricultural soils. Sustainability 10, 2380.

Pantawane, P., Mehere, B., Chahande, R., Potbhare, A., 2020. Phytoreduced copper oxide nanoparticles by using Murraya koenigii leaf extract and its antibacterial activity. Mater. Today Proc. 29, 934–938.

Parikh, P., Zala, D., Makwana, B., 2014. Biosynthesis of Copper Nanoparticles and Their Antimicrobial Activity. Inst Post Studies Res KSV Uni, India, pp. 1–15.

Pasinszki, T., Krebsz, M., 2020. Synthesis and application of zero-valent iron nanoparticles in water treatment, environmental remediation, catalysis, and their biological effects. Nanomaterials 10, 917.

Phugare, S.S., Kalyani, D.C., Surwase, S.N., Jadhav, J.P., 2011. Ecofriendly degradation, decolorization and detoxification of textile effluent by a developed bacterial consortium. Ecotoxicol. Environ. Saf. 74, 1288–1296.

Pickard, S.M., Johnson, T.G., Kuang, K., 2021. Development of High Thermal Conductivity Copper Alloys with Diamond Particle Additions, 2021 23rd European Microelectronics and Packaging Conference & Exhibition (EMPC). IEEE 1–6.

Powell, C., Webster, P., 2019. Copper Alloys, the Corrosion Performance of Metals for the marine Environment: a Basic Guide. CRC Press, pp. 26–41.

Pragyan, R., Pragnya, P., 2019. A comparative study of two different methods for synthesis of copper nanoparticles. E-planet 17, 76–82.

Qi, C., Liu, X., Ma, J., Lin, C., Li, X., Zhang, H., 2016. Activation of peroxymonosulfate by base: implications for the degradation of organic pollutants. Chemosphere 151, 280–288.

Rahmatolahzadeh, R., Aliabadi, M., Motevalli, K., 2017. Cu and CuO nanostructures: facile hydrothermal synthesis, characterization and photocatalytic activity using new starting reagents. J. Mater. Sci. Mater. Electron. 28, 148–156.

Rajesh, K., Ajitha, B., Reddy, Y.A.K., Suneetha, Y., Reddy, P.S., 2018. Assisted green synthesis of copper nanoparticles using Syzygium aromaticum bud extract: physical, optical and antimicrobial properties. Optik 154, 593–600.

Rajeshkumar, S., Menon, S., Kumar, S.V., Tambuwala, M.M., Bakshi, H.A., Mehta, M., Satija, S., Gupta, G., Chellappan, D.K., Thangavelu, L., 2019. Antibacterial and antioxidant potential of biosynthesized copper nanoparticles mediated through Cissus arnotiana plant extract. J. Photochem. Photobiol. B Biol. 197, 111531.

Ramanathan, R., Bhargava, S.K., Bansal, V., 2011. Biological Synthesis of Copper/copper Oxide Nanoparticles. Chemeca. Citeseer, pp. 1–8.

Ramanathan, R., Field, M.R., O'Mullane, A.P., Smooker, P.M., Bhargava, S.K., Bansal, V., 2013. Aqueous phase synthesis of copper nanoparticles: a link between heavy metal resistance and nanoparticle synthesis ability in bacterial systems. Nanoscale 5, 2300–2306.

Raut, S.S., Kamble, S.P., Kulkarni, P.S., 2016. Efficacy of zero-valent copper (Cu0) nanoparticles and reducing agents for dechlorination of mono chloroaromatics. Chemosphere 159, 359–366.

Rebai, I., Fernandes, J.O., Azzouz, M., Benmohammed, K., Bader, G., Benmbarek, K., Cunha, S.C., 2021. Urinary bisphenol levels in plastic industry workers. Environ. Res. 202, 111666.

Rehman, K., Shahzad, T., Sahar, A., Hussain, S., Mahmood, F., Siddique, M.H., Siddique, M.A., Rashid, M.I., 2018. Effect of reactive black 5 azo dye on soil processes related to C and N cycling. PeerJ 6, e4802.

Routoula, E., Patwardhan, S.V., 2020. Degradation of anthraquinone dyes from effluents: a review focusing on enzymatic dye degradation with industrial potential. Environ. Sci. Technol. 54, 647–664.

Sadrolhosseini, A.R., Mahdi, M.A., Alizadeh, F., Rashid, S.A., 2019. Laser ablation technique for synthesis of metal nanoparticle in liquid. Laser Technology and its Applications.

Saha, T.K., Das, R., 2018. Progress in synthesis of propargylamine and its derivatives by nanoparticle catalysis via A3 coupling: a decade update. ChemistrySelect 3, 147–169.

Salam, M., Kosa, S., Al-Nahdi, N., Owija, N., 2019. Removal of Acid Red dye from aqueous solution using zero-valent copper and zero-valent zinc nanoparticles. Desalination Water Treat. 141, 310–320.

Salvadori, M.R., Ando, R.A., Oller Do Nascimento, C.A., Correa, B., 2014. Bioremediation from wastewater and extracellular synthesis of copper nanoparticles by the fungus Trichoderma koningiopsis. Journal of Environmental Science and Health, Part A 49, 1286–1295.

Salvadori, M.R., Lepre, L.F., Ando, R. m A., Oller do Nascimento, C.A., Corrêa, B., 2013. Biosynthesis and uptake of copper nanoparticles by dead biomass of Hypocrea lixii isolated from the metal mine in the Brazilian Amazon region. PLoS One 8, e80519.

Sambiagio, C., Marsden, S.P., Blacker, A.J., McGowan, P.C., 2014. Copper catalysed Ullmann type chemistry: from mechanistic aspects to modern development. Chem. Soc. Rev. 43, 3525–3550.

Seku, K., Reddy Ganapuram, B., Pejjai, B., Mangatayaru Kotu, G., Golla, N., 2018. Hydrothermal synthesis of Copper nanoparticles, characterization and their biological applications. Int. J. Nano Dimens. (IJND) 9, 7–14.

Serra, A., Valles, E., 2018. Advanced electrochemical synthesis of multicomponent metallic nanorods and nanowires: fundamentals and applications. Appl. Mater. Today 12, 207–234.

Shahzeydi, A., Ghiaci, M., Farrokhpour, H., Shahvar, A., Sun, M., Saraji, M., 2019. Facile and green synthesis of copper nanoparticles loaded on the amorphous carbon nitride for the oxidation of cyclohexane. Chem. Eng. J. 370, 1310–1321.

Sharma, R., Gupta, H., 2021. Green synthesis of silver, copper and gold nanoparticles using Terminalia arjuna bark and their effect on seed germination. Nanosci. Nanotechnol. - Asia 11, 243–247.

Shen, W., Mu, Y., Wang, B., Ai, Z., Zhang, L., 2017. Enhanced aerobic degradation of 4-chlorophenol with iron-nickel nanoparticles. Appl. Surf. Sci. 393, 316–324.

Shi, S.-L., Buchwald, S.L., 2015. Copper-catalysed selective hydroamination reactions of alkynes. Nat. Chem. 7, 38–44.

Shikha, J., Ankita, J., Kachhawah, P., Devra, V., 2015. Synthesis and size control of copper nanoparticles and their catalytic application. Trans. Nonferrous Metals Soc. China 25, 3995–4000.

Shobha, G., Moses, V., Ananda, S., 2014. Biological synthesis of copper nanoparticles and its impact. Int. J. Pharm. Sci. Invent 3, 6–28.

Sierra-Ávila, R., Pérez-Alvarez, M., Valdez-Garza, J., Avila-Orta, C.A., Jiménez-Regalado, E.J., Mata-Padilla, J.M., Soto-Castruita, E., Cadenas-Pliego, G., 2018. Synthesis and thermomechanical characterization of nylon 6/Cu nanocomposites produced by an ultrasound-assisted extrusion method. Adv. Mater. Sci. Eng.

Soganci, T., Ayranci, R., Harputlu, E., Ocakoglu, K., Acet, M., Farle, M., Unlu, C.G., Ak, M., 2018. An effective non-enzymatic biosensor platform based on copper nanoparticles decorated by sputtering on CVD graphene. Sensor. Actuator. B Chem. 273, 1501–1507.

Soomro, R.A., Sherazi, S.H., Memon, N., Shah, M., Kalwar, N., Hallam, K.R., Shah, A., 2014. Synthesis of air stable copper nanoparticles and their use in catalysis. Adv. Mater. Lett. 5, 191–198.

Suárez-Cerda, J., Espinoza-Gómez, H., Alonso-Núñez, G., Rivero, I.A., Gochi-Ponce, Y., Flores-López, L.Z., 2017. A green synthesis of copper nanoparticles using native cyclodextrins as stabilizing agents. J. Saudi Chem. Soc. 21, 341–348.

Suresh, Y., Annapurna, S., Bhikshamaiah, G., Singh, A., 2013. Characterization of green synthesized copper nanoparticles: a novel approach. International Conference on Advanced Nanomaterials & Emerging Engineering Technologies. IEEE 63–67.

Thiruvengadam, M., Chung, I.-M., Gomathi, T., Ansari, M.A., Khanna, V.G., Babu, V., Rajakumar, G., 2019. Synthesis, characterization and pharmacological potential of green synthesized copper nanoparticles. Bioproc. Biosyst. Eng. 42, 1769–1777.

Tkaczyk, A., Mitrowska, K., Posyniak, A., 2020. Synthetic organic dyes as contaminants of the aquatic environment and their implications for ecosystems: a review. Sci. Total Environ. 717, 137222.

Tokoi, Y., Nagasawa, S., Suematsu, H., Cho, H.B., Nakayama, T., Niihara, K., 2013. Preparation of copper nanoparticles by pulsed wire discharge in water. Materials Science Forum. Trans Tech Publ 121–124.

Tyurnina, A., Shur, V.Y., Kozin, R., Kuznetsov, D., Pryakhina, V., Burban, G., 2014. Synthesis and investigation of stable copper nanoparticle colloids. Phys. Solid State 56, 1431–1437.

Umer, A., Naveed, S., Ramzan, N., Rafique, M.S., Imran, M., 2014. A green method for the synthesis of copper nanoparticles using L-ascorbic acid. Materia 19, 197–203.

Vajargah, M.F., 2021. A review on the effects of heavy metals on aquatic animals. Environ. Sci. 2.

Varshney, R., Bhadauria, S., Gaur, M., Pasricha, R., 2011. Copper nanoparticles synthesis from electroplating industry effluent. Nano. Biomed. Eng. 3, 115–119.

Varshney, R., Bhadauria, S., Gaur, M.S., Pasricha, R., 2010. Characterization of copper nanoparticles synthesized by a novel microbiological method. JOM (J. Occup. Med.) 62, 102–104.

Wan, J., Ma, J., Zhang, Y., Xia, Y., Hong, L., Yang, C., 2021. Improved antioxidative performance of a water-soluble copper nanoparticle@fullerenol composite formed via photochemical reduction. New J. Chem. 45, 17660–17666.

Wang, D., Xu, H., Ma, J., Giannakis, S., Lu, X., Chi, H., Song, S., Qi, J., 2019a. Enhanced mineralization of atrazine by surface induced hydroxyl radicals over light-weight granular mixed-quartz sands with ozone. Water Res. 149, 136–148.

Wang, K., Yang, L., Zhao, W., Cao, L., Sun, Z., Zhang, F., 2017. A facile synthesis of copper nanoparticles supported on an ordered mesoporous polymer as an efficient and stable catalyst for solvent-free sonogashira coupling Reactions. Green Chem. 19, 1949–1957.

Wang, Q., Cao, Y., Zeng, H., Liang, Y., Ma, J., Lu, X., 2019b. Ultrasound-enhanced zero-valent copper activation of persulfate for the degradation of bisphenol AF. Chem. Eng. J. 378, 122143.

Wang, S., Kuo, Y., Huang, Y., Huang, C., Kao, C., 2015. Bioremediation of 1, 2-dichloroethane contaminated groundwater: microcosm and microbial diversity studies. Environ. Pollut. 203, 97–106.

Wang, X.Y., Chen, C., Chang, Y., Liu, H.L., 2009. Dechlorination of chlorinated methanes by Pd/Fe bimetallic nanoparticles. J. Hazard Mater. 161, 815–823.

Wen, G., Wang, S.-J., Ma, J., Huang, T.-L., Liu, Z.-Q., Zhao, L., Xu, J.-L., 2014. Oxidative degradation of organic pollutants in aqueous solution using zero valent copper under aerobic atmosphere condition. J. Hazard Mater. 275, 193–199.

Wu, S.-J., Liou, T.-H., Mi, F.-L., 2009. Synthesis of zero-valent copper-chitosan nanocomposites and their application for treatment of hexavalent chromium. Bioresour. Technol. 100, 4348–4353.

Xu, D., Bai, Y., Li, Z., Guo, Y., Bai, L., 2018. Enhanced photodegradation ability of solvothermally synthesized metallic copper coated ZnO microrods. Colloids Surf. A Physicochem. Eng. Asp. 548, 19–26.

Xu, L., Yang, Y., Li, W., Tao, Y., Sui, Z., Song, S., Yang, J., 2019. Three-dimensional macroporous graphene-wrapped zero-valent copper nanoparticles as efficient micro-electrolysis-promoted Fenton-like catalysts for metronidazole removal. Sci. Total Environ. 658, 219–233.

Yallappa, S., Manjanna, J., Sindhe, M., Satyanarayan, N., Pramod, S., Nagaraja, K., 2013. Microwave assisted rapid synthesis and biological evaluation of stable copper nanoparticles using T. arjuna bark extract. Spectrochim. Acta Mol. Biomol. Spectrosc. 110, 108–115.

Yamaguchi, R., Kurosu, S., Suzuki, M., Kawase, Y., 2018. Hydroxyl radical generation by zero-valent iron/Cu (ZVI/Cu) bimetallic catalyst in wastewater treatment: heterogeneous Fenton/Fenton-like reactions by Fenton reagents formed in-situ under oxic conditions. Chem. Eng. J. 334, 1537–1549.

Yang, M., Mao, M., He, Y., Zhou, J., Ge, Y., Song, G., 2019. Fabrication of hybrids of zeolitic imidazolate frameworks supported zero-valent copper nanoparticles as a non-noble catalyst with high efficiency. Micro & Nano Lett. 14, 163–167.

Yanson, A.I., Rodriguez, P., Garcia-Araez, N., Mom, R.V., Tichelaar, F.D., Koper, M.T., 2011. Cathodic corrosion: a quick, clean, and versatile method for the synthesis of metallic nanoparticles. Angew. Chem. Int. Ed. 50, 6346–6350.

Yu, Y., Yu, Z., Chen, H., Han, Y., Xiang, M., Chen, X., Ma, R., Wang, Z., 2019. Tetrabromobisphenol A: disposition, kinetics and toxicity in animals and humans. Environ. Pollut. 253, 909–917.

Yuan, Y., Li, H., Lai, B., Yang, P., Gou, M., Zhou, Y., Sun, G., 2014. Removal of high-concentration CI acid orange 7 from aqueous solution by zerovalent iron/copper (Fe/Cu) bimetallic particles. Ind. Eng. Chem. Res. 53, 2605–2613.

Zhang, J., Guo, J., Wu, Y., Lan, Y., Li, Y., 2017a. Efficient activation of ozone by zero-valent copper for the degradation of aniline in aqueous solution. J. Taiwan Inst. Chem. Eng. 81, 335–342.

Zhang, L., Fu, Y., Wang, Z., Zhou, G., Zhou, R., Liu, Y., 2021. Removal of diclofenac in water using peracetic acid activated by zero valent copper. Separ. Purif. Technol. 276, 119319.

Zhang, N., Xue, C., Wang, K., Fang, Z., 2020a. Efficient oxidative degradation of fluconazole by a heterogeneous Fenton process with Cu-V bimetallic catalysts. Chem. Eng. J. 380, 122516.

Zhang, T., Yang, Y., Li, X., Yu, H., Wang, N., Li, H., Du, P., Jiang, Y., Fan, X., Zhou, Z., 2020b. Degradation of sulfamethazine by persulfate activated with nanosized zero-valent copper in combination with ultrasonic irradiation. Separ. Purif. Technol. 239, 116537.

Zhang, Y., Fan, J., Yang, B., Huang, W., Ma, L., 2017b. Copper–catalyzed activation of molecular oxygen for oxidative destruction of acetaminophen: the mechanism and superoxide-mediated cycling of copper species. Chemosphere 166, 89–95.

Zhao, C., Chen, W., 2019. A review for tannery wastewater treatment: some thoughts under stricter discharge requirements. Environ. Sci. Pollut. Control Ser. 26, 26102–26111.

Zheng, W., Liu, Y., Liu, W., Ji, H., Li, F., Shen, C., Fang, X., Li, X., Duan, X., 2021. A novel electrocatalytic filtration system with carbon nanotube supported nanoscale zerovalent copper toward ultrafast oxidation of organic pollutants. Water Res. 194, 116961.

Zhou, L., Wang, S., Ma, H., Ma, S., Xu, D., Guo, Y., 2015. Size-controlled synthesis of copper nanoparticles in supercritical water. Chem. Eng. Res. Des. 98, 36–43.

Zhou, P., Liu, B., Zhang, J., Zhang, Y., Zhang, G., Wei, C., Liang, J., Liu, Y., Zhang, W., 2016. Radicals induced from peroxomonosulfate by nanoscale zero-valent copper in the acidic solution. Water Sci. Technol. 74, 1946–1952.

Zhu, H-t, Zhang, C-y, Yin, Y-s, 2004. Rapid synthesis of copper nanoparticles by sodium hypophosphite reduction in ethylene glycol under microwave irradiation. J. Cryst. Growth 270, 722–728.

Zhu, H., Zhang, C., Yin, Y., 2005. Novel. Synthesis of copper nanoparticles: influence of the synthesis conditions on the particle size. Nanotechnology 16, 3079.

Žvab, U., Kukulin, D.S., Fanetti, M., Valant, M., 2021. Bioremediation of copper polluted wastewater-like nutrient media and simultaneous synthesis of stable copper nanoparticles by a viable green alga. J. Water Proc. Eng. 42, 102123.